

**Contract No:**

This document was prepared in conjunction with work accomplished under Contract No. DE-AC09-08SR22470 with the U.S. Department of Energy (DOE) Office of Environmental Management (EM).

**Disclaimer:**

This work was prepared under an agreement with and funded by the U.S. Government. Neither the U. S. Government or its employees, nor any of its contractors, subcontractors or their employees, makes any express or implied:

- 1 ) warranty or assumes any legal liability for the accuracy, completeness, or for the use or results of such use of any information, product, or process disclosed; or
- 2 ) representation that such use or results of such use would not infringe privately owned rights; or
- 3) endorsement or recommendation of any specifically identified commercial product, process, or service.

Any views and opinions of authors expressed in this work do not necessarily state or reflect those of the United States Government, or its contractors, or subcontractors.



# Historical Scaling Performance from Laboratory to Full Scale for the Defense Waste Processing Facility's Chemical Process Cell

**D. P. Lambert**

**M. R. Poirier**

April 2019

SRNL-STI-2017-00073, Revision 0



## **DISCLAIMER**

This work was prepared under an agreement with and funded by the U.S. Government. Neither the U.S. Government or its employees, nor any of its contractors, subcontractors or their employees, makes any express or implied:

1. warranty or assumes any legal liability for the accuracy, completeness, or for the use or results of such use of any information, product, or process disclosed; or
2. representation that such use or results of such use would not infringe privately owned rights; or
3. endorsement or recommendation of any specifically identified commercial product, process, or service.

Any views and opinions of authors expressed in this work do not necessarily state or reflect those of the United States Government, or its contractors, or subcontractors.

**Printed in the United States of America**

**Prepared for  
U.S. Department of Energy**

**Keywords:** *DWPF, flowsheet, formic acid, scaling, CPC*

**Retention:** *Permanent*

# Historical Scaling Performance from Laboratory to Full Scale for the Defense Waste Processing Facility's Chemical Process Cell

D. P. Lambert

M. R. Poirier

April 2019

---

Prepared for the U.S. Department of Energy under contract number DE-AC09-08SR22470.



**REVIEWS AND APPROVALS**

## AUTHORS:

---

D. P. Lambert, Process Technology Programs	Date
--	------

## TECHNICAL REVIEW:

---

J. R. Zamecnik, Process Technology Programs, Reviewed per E7 2.60	Date
---	------

---

M. E. Stone, Wasteform Processing Technologies	Date
--	------

## APPROVAL:

---

F. M. Pennebaker, Manager Liquid Waste Program	Date
---	------

---

S. D. Fink, Director, Chemical Processing Technologies	Date
--	------

---

E. J. Freed, Manager DWPF/Saltstone Facility Engineering	Date
---	------

## ACKNOWLEDGEMENTS

The data used in the report was collected by a number of people and they are acknowledged below:

Roger Mahannah maintains spreadsheets with DWPF analytical data. The data for SRAT receipt, SRAT product and SME product were extracted from the spreadsheets labeled “All SRAT SME MFT SB6.xls” and “All SRAT SME MFT SB8 (671-773).xlsx”.

The DWPF CPC engineers maintain spreadsheets containing the acid calculations from each run. The data needed for the acid calculations were extracted from “SRAT Acid SB8.xlsm” and “Acid SB6 566-750.xls”. These data together with SRAT product analysis data were used to calculate the anion destruction factors used to predict REDOX.

A great deal of DWPF processing data was extracted from the PI process data archiving software by Scot Beck. These data were used for many of the graphs and tables in the report.

Data was also extracted from dozens of SRNL reports. The authors are thanked for documenting these data. The data used most extensively came from SB6 and SB8, so special thanks to John Pareizs, David Newell, David Koopman, and their coauthors.

This document is a response to a question from a recommendation from the Alternate Reductant Independent Technology Review performed by Lou Papouchado, Sharon Marra, and Jay Roach, which was completed in January 2017.

## EXECUTIVE SUMMARY

The Defense Waste Processing Facility (DWPF) is planning to modify the chemical processing flowsheet by replacing formic acid with glycolic acid in the Chemical Process Cell (CPC) Sludge Receipt and Adjustment Tank (SRAT) and Slurry Mix Evaporator (SME). The replacement of formic acid with glycolic acid virtually eliminates the CPC's largest flammability hazards, catalytic hydrogen and ammonia.

Prior to DWPF startup, full, semiworks, pilot and laboratory scale testing were completed to understand the chemistry and engineering of radioactive waste processing. Actual waste experiments up to 25-L were performed. Since the first DWPF radioactive sludge batch processed in March 1996, a Nitric-Formic Acid operating window has been developed for each of the eleven sludge batches based on ~4-L simulant experiments and a single ~1-L radioactive demonstration. Although pilot-scale testing was instrumental in the initial design and flowsheet development for the DWPF, pilot-scale testing has not been used to develop the CPC operating window during radioactive processing. This is true even for the incorporation of new salt processing effluents into the DWPF process (i.e., Actinide Removal Process in 2007 and Modular Caustic-Side Solvent Extraction Unit in 2008).

This report concludes that the process chemistry is essentially the same in simulant testing, in an actual waste demonstration, and during the DWPF processing of each sludge batch. Throughout testing and operation of the Nitric-Formic Acid flowsheet the chemistry has been essentially the same regardless of scale of testing or operation. In both laboratory experiments and the DWPF, mixing and heat transfer are adequate to mix immiscible liquids, organics and insoluble solids. Rheology of the chemical simulants, in general, do not adequately represent real waste other than to provide an indicator of the behavior of real sludge. Similarly, for mass transfer processes like mercury stripping and recovery, simulant small scale testing will likely require some larger pilot testing to better represent DWPF operation. As a result, larger scale testing was performed in the development of the Nitric-Formic Acid and the Nitric-Glycolic Acid flowsheets.

Extensive testing has been completed to develop the Nitric-Glycolic Acid CPC flowsheet. Over 100 simulations have been completed to understand the keys to chemical processing. Testing has been completed at three different scales including laboratory testing in 4-L and 22-L processing equipment along with testing in geometrically scaled 220-L (~1/216<sup>th</sup>) pilot-scale equipment. The testing utilized non-radioactive simulants of various sludge batches as well as a matrix of simulants designed to bound the compositional range of sludge solids. In addition, a small number of 1-L tests have been performed with samples of radioactive tank waste. The larger scale testing was used to validate the equivalency of the smaller scale testing protocol.

A Sludge Batch (SB) 9 simulant was used to develop the first sludge batch specific Nitric-Glycolic Acid CPC operating window. CPC simulations were completed using sludge simulant, Strip Effluent Feed Tank simulant and Precipitate Reactor Feed Tank simulant. Ten sludge-only SRAT cycles and four SRAT/SME cycles were completed. In addition, one actual SB9 sludge-only SRAT and SME cycle was completed as part of the SB9 flowsheet process development.

The same testing philosophy that is used for the development of each sludge batch's Nitric-Formic Acid flowsheet is also recommended for development of an operating window for the Nitric-Glycolic Acid flowsheet, namely that development be based on ~4-L simulant experiments and a ~4-L radioactive demonstration. The 4-L radioactive experiment (rather than 1-L) allows more analyses (particularly rheology) to be completed to better understand the extended processing that will be needed after the Salt Waste Processing Facility (SWPF) startup. The recommended processing target for the actual waste experiment and for DWPF processing is based on maximizing solids concentration (to maximize melter efficiency) and mercury removal.

## TABLE OF CONTENTS

LIST OF TABLES .....	ix
LIST OF FIGURES .....	x
LIST OF ABBREVIATIONS .....	xi
1.0 Introduction .....	1
1.1 Initial Pilot Testing to Support DWPF Startup.....	1
1.2 Cold Chemical Testing in DWPF .....	2
1.3 Qualification of Nitric-Formic Acid Flowsheets.....	3
1.4 Development of the Nitric-Glycolic Acid Flowsheet.....	3
1.5 Scale-up Testing of the Nitric-Glycolic Acid Flowsheet .....	4
1.6 Independent Technical Review of the Nitric-Glycolic Acid Flowsheet.....	4
1.7 Scope of This Work.....	4
1.8 Deliverable .....	4
2.0 Quality Assurance .....	4
3.0 Results and Discussion .....	5
3.1 Scaling Discussions .....	5
3.2 Process Window Chemistry .....	6
3.2.1 Nitrite Destruction .....	7
3.2.2 Hydrogen Generation.....	9
3.3 Anion Destruction .....	12
3.3.1 Formate Destruction .....	13
3.3.2 Oxalate Destruction .....	14
3.3.3 Nitrite to Nitrate Conversion .....	15
3.4 Reduction/Oxidation (REDOX) .....	16
3.5 Mercury Stripping .....	17
3.6 Offgas Chemistry .....	18



3.6.1 Offgas Species .....	19
3.6.2 Oxygen Depletion and Nitrogen/Oxygen Ratio.....	20
3.6.3 Oxides of Nitrogen Generation.....	22
3.6.4 Carbon Dioxide Generation .....	23
3.7 Physical Parameters Important to Processing.....	23
3.7.1 Mixing and Heat Transfer.....	23
3.7.2 Foam/Antifoam.....	27
3.8 Processing Window for the Nitric-Glycolic Acid Flowsheet.....	28
4.0 Conclusions.....	29
5.0 Recommendations.....	30
6.0 References.....	31
Appendix A -- Email Requesting This Task.....	A-1
Appendix B – Offgas Hydrogen Data.....	B-1
Appendix C —Physical Parameters of Interest.....	C-1
Appendix D —Cavern Mixing Analysis.....	D-1

**LIST OF TABLES**

Table 1-1. List of IDMS Runs .....	2
Table 2-1. Experiments and DWPF Batches Used in This Analysis .....	5
Table 3-1. SRAT and SME Relative Scaling* .....	6
Table 3-2. SRAT Product Nitrite Concentration, mg/kg .....	8
Table 3-3. SRAT Hydrogen Peak Data for Nitric-Formic Acid Flowsheet.....	10
Table 3-4. Peak Catalytic Hydrogen Comparison Between SRNL and DWPF for the SRAT Cycle.....	12
Table 3-5. SRAT Formate Loss and Correction Factor Data.....	14
Table 3-6. SB8 SRAT Oxalate Destruction and Correction Factor Data.....	14
Table 3-7. SRAT Nitrite to Nitrate Conversion and Nitrate Correction Factor Data .....	15
Table 3-8. Predicted and Measured Formate, Nitrate, Oxalate, and Mn for Predicting REDOX in SRAT Product Sample.....	16
Table 3-9. Predicted SRAT Product REDOX at 36% Waste Loading .....	17
Table 3-10. SRAT Product Mercury Data .....	18
Table 3-11. SRAT and SME Antifoam Strategy for Nitric-Glycolic Acid and Nitric-Formic Acid Flowsheets, gallons undiluted antifoam .....	27
Table 3-12. Calculated Boiling Flux in SRAT for Scaled Experiments .....	28

**LIST OF FIGURES**

Figure 3-1. Example of a Sludge Batch Operating Window .....	7
Figure 3-2. SRAT Hydrogen Generation Peaks Due to Rh and Ru.....	8
Figure 3-3. SB6 SRAT Hydrogen Concentration, Volume Percentage.....	10
Figure 3-4. SB8 SRAT Hydrogen Concentration, Volume Percentage.....	11
Figure 3-5. N <sub>2</sub> O, CO <sub>2</sub> , and H <sub>2</sub> profile from SRNL SC-6 and DWPF Batch 474 .....	12
Figure 3-6. Calculated Offgas Flowrates, scfm for DWPF Batch 535 .....	20
Figure 3-7. Oxygen Profile for Selected SB6 Experiments and DWPF Batches.....	21
Figure 3-8. Oxygen Profile for Selected SB8 Experiments and DWPF Batches.....	21
Figure 3-9. SB6 535 Oxygen Depletion, Nitrogen and Oxygen Offgas Flow, scfm .....	22
Figure 3-10. Ekato Method for Predicting Mixing Speed at Different Scale .....	23
Figure 3-11. SB6 Calculated Heat Transfer Coefficient for DWPF SRAT Steam Coils.....	25
Figure 3-12. SB8 Calculated Heat Transfer Coefficient for DWPF SRAT Steam Coils.....	25
Figure 3-13. SB8 Laboratory Scale Calculated Heat Transfer Coefficient for Heating Rods .....	26

**LIST OF ABBREVIATIONS**

AFP	Alpha Finishing Process (feed from SWPF to PRFT)
ASP	Alpha Strike Process (feed from SWPF to PRFT)
ARP	Actinide Removal Process (feed from ARP to PRFT)
CF	Correction Factor
CPC	Chemical Processing Cell
DWPF	Defense Waste Processing Facility
ELN	Electronic Lab Notebook
FAVC	Formic Acid Vent Condenser
FTIR	Fourier Transform Infrared Spectrometer (or Spectroscopy)
GC	Gas Chromatograph (or Chromatography)
HM	H Modified PUREX Process (HM)
IDMS	Integrated DWPF Melter System (1/5 <sup>th</sup> scale CPC, 1/9 <sup>th</sup> scale melter)
ITR	Independent Technology Review
ITP	In Tank Precipitation
KMA	Koopman Minimum Acid
MCU	Modular Caustic-Side Solvent Extraction Unit
MWWT	Mercury Water Wash Tank
NA	Not Applicable
NO <sub>x</sub>	NO + NO <sub>2</sub>
NR	Not Requested
N <sub>y</sub> O <sub>x</sub>	NO + NO <sub>2</sub> + N <sub>2</sub> O
PHA	Precipitate Hydrolysis Aqueous
PRFT	Precipitate Reactor Feed Tank (ARP or AFP Feed Tank)
PUREX	Plutonium URanium EXtraction
REDOX	REDuction/OXidation
SB	Sludge Batch
scfm	Standard Cubic Feet per Minute
SEFT	Strip Effluent Feed Tank
SL	Standard Liter
SME	Slurry Mix Evaporator
SMECT	Slurry Mix Evaporator Condensate Tank
SRAT	Sludge Receipt Adjustment Tank
SRNL	Savannah River National Laboratory
SRR	Savannah River Remediation
TNX	TNX was in T-Area at the Savannah River Site
TPB	Tetraphenylborate
TTR	Technical Task Request

## 1.0 Introduction

Initial development of the Defense Waste Processing Facility (DWPF) Chemical Process Cell (CPC) flowsheet was for a coupled process that combined well-washed sludge and tetraphenylborate (TPB) precipitate hydrolysis aqueous (PHA) product. The PHA product was to be pretreated in the DWPF Salt Processing Cell prior to blending with the sludge in the SRAT and the frit in the SME. Development of this flowsheet and design of DWPF included a one-fifth pilot-scale facility at TNX operated with non-radioactive simulants containing all species except radionuclides, and full-scale simulant testing at TNX that also excluded noble metals and mercury. The initial pilot testing is discussed in Section 1.1.

The DWPF coupled flowsheet was revised multiple times due to emerging issues such as organic deposits and poor nitrite destruction in the Salt Cell Process and excessive generation of flammable gases (hydrogen and ammonia) in CPC processing. The last CPC experiment in the Integrated DWPF Melter System (IDMS) pilot-plant was completed in April 1995 for the development of sludge/PHA “coupled” operation.

However, the TPB process in the H-Tank Farm that generated the precipitate was cancelled because of excessive benzene generation during precipitation. Thus, the sludge/TPB coupled process was never implemented in DWPF radioactive processing.<sup>1</sup> The IDMS pilot-plant was shut down prior to the radioactive startup of DWPF so pilot-scale testing has not been used in the development of any of the radioactive operating windows for DWPF. DWPF began radioactive operation in March 1996 using a sludge-only process (i.e. sludge without additions of the TPB product). The initial sludge-only flowsheet replaced the formic acid and copper expected from the PHA product after processing in the DWPF salt cell with a formic acid/copper stream, which was added to the SRAT at boiling.

Testing with nonradioactive simulants in DWPF was completed prior to radioactive startup. Testing was designed to demonstrate the coupled processing of sludge and PHA. The cold chemical testing with simulant in DWPF is discussed in Section 1.2.

The sludge only flowsheet, like all subsequent nitric and formic acid flowsheets, was developed based on 4-L simulant experiments and a 1-L radioactive experiment. No pilot-scale testing was completed in developing processing windows for each sludge batch. This is true even after the radioactive startup of the Actinide Removal Process\* (ARP) in 2007 and the Modular Caustic-Side Solvent Extraction Unit (MCU) in 2008. The development of the flowsheet and qualification of the sludge batch for the Nitric-Formic Acid process is discussed in Section 1.3.

An extensive testing program was completed to develop a new flowsheet to eliminate the use of formic acid in the CPC. This virtually eliminated the generation of hydrogen and ammonia, two flammability hazards in DWPF. The development of a Nitric-Glycolic Acid flowsheet and the qualification of the Sludge Batch 9 (SB9) for the Nitric-Glycolic Acid process are discussed in Section 1.4.

### 1.1 Initial Pilot Testing to Support DWPF Startup

IDMS was designed and constructed as a semiworks pilot plant for the DWPF CPC, melter, and offgas treatment systems. IDMS was built as a 1/5<sup>th</sup> scale CPC and 1/9<sup>th</sup> scale melter. After the discovery of noble metal-catalyzed dehydrogenation of formic acid hydrogen and ammonia generation, IDMS was modified to increase the air purge due to the high hydrogen generation. Twenty-two IDMS DWPF campaigns were completed over a period of seven years as summarized in Table 1-1. This included ten campaigns with noble metals and mercury, three with mercury but no noble metals and nine without added noble metals or mercury. Twenty campaigns were completed with PHA (the other two were sludge only campaigns without noble metals and mercury).

---

\* Post SWPF startup, feed for the PRFT will come from the Alpha Finishing Process (AFP) or Alpha Strike Process (ASP)

IDMS testing was designed to verify the processing as predicted in smaller scale experiments prior to the cold chemical testing in DWPF. It was also designed to demonstrate the effect of mixing, foaming, mercury stripping, and other parameters that were hard to scale up. Campaigns were completed with simulants of Batch 1 sludge, a blend of Plutonium Uranium Extraction (PUREX) and H Modified PUREX (HM) sludge, HM sludge, PUREX sludge and with Hanford sludge (not included in table below). Although the testing was very valuable in understanding the processing of sludge with noble metals and mercury, this testing was not used to develop any of the radioactive flowsheets for DWPF radioactive processing.

**Table 1-1. List of IDMS Runs**

Run	Sludge Type	PHA Type	Noble Metals?	Mercury?	Report
Sludge Only#1	Batch 1	None	No	No	WSRC-RP-89-0321 <sup>2</sup>
Sludge Only#2	Batch 1	None	No	No	
PHA#1	Blend	HAN	No	No	WSRC-TR-90-0131 <sup>3</sup>
PHA#2	Blend	HAN	No	No	
PHA#3	Blend	HAN	No	No	
HG#1	Batch	HAN	No	Yes	WSRC-TR-91-0063 <sup>4</sup>
HG#2	Batch	HAN	No	Yes	
HG#3	Batch	HAN	No	Yes	
Blend#1	Blend	HAN	No	No	WSRC-TR-91-400 <sup>5</sup>
Blend#2	Blend	HAN	No	No	
Blend#3	Blend	HAN	Yes	Yes	WSRC-TR-93-593 <sup>6</sup>
HM#1	HM	HAN	Yes	Yes	
HM#2	HM	HAN	Yes	Yes	Not Documented
HM#3	HM	HAN	Yes	Yes	
PX#1	PUREX	HAN	Yes	Yes	
PX#2	PUREX	HAN	Yes	Yes	
HM#4	HM	HAN	Yes	Yes	WSRC-TR-92-0492 <sup>7</sup>
PX#3	PUREX	HAN	Yes	Yes	
PX#4	PUREX	Late Wash	Yes	Yes	WSRC-TR-92-0492 <sup>7</sup>
PX#5	PUREX	Late Wash	Yes	Yes	
PX#6	PUREX	Late Wash	Yes	Yes	WSRC-TR-94-0556 <sup>8</sup>
PX#7	PUREX	Late Wash	Yes	Yes	WSRC-TR-94-8000 <sup>9</sup>

## 1.2 Cold Chemical Testing in DWPF

Prior to the start of Radioactive Operations in 1996, DWPF underwent an extensive Startup Test Program. This test program consisted of Integrated Water Runs, Chemical Runs and Waste Qualification Runs. The Chemical Runs consisted of three SRAT/SME batches with blend sludge, PHA, without noble metals, and without mercury. The Waste Qualification Runs consisted of 13 SRAT/SME batches with bounding sludges, PHA, without noble metals, without mercury. The Proficiency Runs consisted of two SRAT/SME batches with SB1A sludge simulant, noble metals, mercury, formic acid and copper mixed with water to replace PHA.<sup>10</sup> This was followed by DWPF radioactive startup in 1996 with SB1A sludge along with the formic acid, and copper mixed with water.<sup>10-11</sup>

Except for the Proficiency Runs, the DWPF simulant runs were very different from radioactive SB1A processing as only three included noble metals and the rest included DWPF Salt Processing Cell produced PHA (rather than the formic acid, copper, water solution used in SB1A radioactive processing).

### 1.3 Qualification of Nitric-Formic Acid Flowsheets

Laboratory scale testing with simulants and one actual waste demonstration were completed in developing a radioactive CPC processing window for each Sludge Batch (SB) that has been successfully processed in DWPF (SB1A, SB1B<sup>12</sup>, SB2<sup>13-14</sup>, SB3<sup>15-16</sup>, SB4<sup>17-18</sup>, SB5<sup>19-20</sup>, SB6<sup>21-22</sup>, SB7<sup>23</sup>, SB7B<sup>24-25</sup>, SB8<sup>26-27</sup>, SB9<sup>28-29</sup>). In developing processing flowsheets for each of these sludge batches, the processing window was bounded by inadequate nitrite destruction if too little acid was added (to ensure the hydrogen peak generation occurs in the SRAT where the purge is biggest) and excessive hydrogen in the CPC if too much acid was added. Testing was completed with conservatively high noble metal additions to ensure the peak hydrogen generation in simulant tests was conservative.

In addition to the development of a processing window for each sludge batch, processing changes and improvements were developed to incorporate additional waste streams. The following changes were developed to improve CPC processing in DWPF:

- An interim flowsheet with a nitric acid sludge-only process combined with synthetic PHA<sup>30</sup> stream containing a copper catalyst and formic acid. (This was an interim flowsheet developed in 1995 as a temporary flowsheet until In Tank Precipitation (ITP) could supply precipitate to the DWPF)
- A sludge-only process without the synthetic PHA stream
- A REDOX adjusted sludge-only process with both nitric and formic acid added at 93 °C
- A coupled flowsheet that combined ARP Precipitate Reactor Feed Tank (PRFT) feed and MCU Strip Effluent Feed Tank (SEFT) material<sup>31</sup>

It should be noted that the DWPF has had processing issues that were not identified during the laboratory scale testing or DWPF testing with simulants. The simulants used in laboratory testing are chemical and not physical simulants. In other words, physical properties such as rheology and foaming may not be well simulated. Actual waste is typically thicker rheologically than the simulant at the same total or insoluble solids concentration. It is extremely important to complete radioactive waste testing since simulants do not duplicate all the waste properties. Measurement of the rheology of SRAT and SME products in actual waste experiments is important for processing.

### 1.4 Development of the Nitric-Glycolic Acid Flowsheet

Roughly one-hundred experiments<sup>32, 33,34,35,36,37,38,39</sup> with simulants and two shielded cells demonstrations with actual waste<sup>40,29</sup> were completed in the development of the Nitric-Glycolic Acid flowsheet for the DWPF CPC. Most of the testing has been completed to simulate sludge-only testing but ten of the experiments have included strip effluent and seven of the experiments have included ARP product. Testing was completed in simulant experiments at the 4-L, 22-L laboratory scale and at the 220- L pilot scale.

For the Nitric-Glycolic Acid flowsheet, testing was not performed at the semiworks scale (Section 1.1) or full-scale (Section 1.2). Hence, no testing at the semiworks scale has been completed in developing the chemical flowsheets for any of the radioactive sludge batches for DWPF.

In addition, laboratory scale testing with simulants and one actual waste demonstration were completed in developing the SB9 CPC flowsheet for DWPF. In developing this flowsheet, the processing window was bounded by thick rheology if too little acid was added and thin rheology if too much acid was added. Testing was completed with conservatively high noble metal additions to ensure the peak hydrogen generation in simulant tests exceeded the hydrogen generation in the actual waste demonstration and in DWPF processing.

### 1.5 Scale-up Testing of the Nitric-Glycolic Acid Flowsheet

Testing was completed at three different scales to demonstrate that the Nitric-Glycolic Acid flowsheet scales from the 4-L lab scale to the 22-L bench scale and 220-L engineering scale.<sup>35</sup> Ten process demonstrations of the sludge-only flowsheet for SRAT and Slurry Mix Evaporator (SME) cycles were performed using Sludge Batch 8 (SB8)-Tank 40 simulant. No ARP product or SEFT material was added during the runs. Six experiments were completed at the 4-L scale, two experiments were completed at the 22-L scale, and two experiments were completed at the 220-L scale. Experiments completed at the 4-L scale (100 and 110% acid stoichiometry) were repeated at the 22-L and 220-L scale for scale comparisons. A report summarized the results of this testing.<sup>35</sup> No testing of the Nitric-Glycolic Acid flowsheet has been completed at the semiworks or DWPF scale.

### 1.6 Independent Technical Review of the Nitric-Glycolic Acid Flowsheet

An Independent Technology Review (ITR) of the Nitric-Glycolic Acid flowsheet was completed January 10-12, 2017.<sup>41</sup> The review identified the need for an evaluation (this report) recommending the basis for scaling the Nitric-Glycolic Acid flowsheet to DWPF without the need for testing in a semiworks or full-scale processing facility.

### 1.7 Scope of This Work

The following work scope applies to this task as described in the request from SRR (Appendix A):<sup>42</sup>

“As discussed in the ‘Background’ section of HLW-DWPF-TTR-2013-0003 Rev. 0, historical performance of small-scale testing has been the basis for scaling from 4-liter testing to full DWPF scale. To address a comment from the ITR of the Nitric-Glycolic Acid flowsheet, please document the scaling performance of historical testing for the Nitric-Formic Acid flowsheet utilizing laboratory scale, Integrated DWPF Melter System (IDMS), scale melter, and DWPF cold and radioactive runs. As part of this documentation, this scaling rationale should be applied to the Nitric-Glycolic Acid flowsheet. This does not require a revision of the Task Technical and Quality Assurance Plan since it is within the scope as defined in SRNL-RP-2012-00762, Rev. 0. This email scope clarification shall be documented in the appropriate SRNL laboratory notebook<sup>37</sup> and included as an attachment to the technical report.”

### 1.8 Deliverable

A stand-alone technical report documenting the historical performance of scaling from laboratory to bench to semiworks to full scale for the DWPF process. Performance is based on the Nitric-Formic Acid flowsheet with the technical basis for extending the scaling process to the Nitric-Glycolic Acid flowsheet.

## 2.0 **Quality Assurance**

No testing was directly performed to support this report. This report utilizes data from previous testing along with DWPF process and analytical data to determine the historical scaling performance from laboratory to DWPF.

DWPF operating data was extracted from the PI Process Book 3.2.0.0. DWPF analytical data was extracted from DWPF analytical data from each of the SRAT-1, SRAT-4, and SME-1 sample sets from each SRAT and SME batch.

To simplify the analysis, two sludge batches were included in this analysis, SB6 and SB8 (SB8 runs are shaded in the tables for clarity throughout this report). Since many DWPF batches were performed for each of these sludge batches, only data from Batches 535, 555, and 565 were included as part of SB6 and only data from Batches 680, 705, and 735 were included as part of SB8. Shielded Cells run SC-10, a SB6 run and Shielded Cells run SC-14, an SB8 run were included in the analysis. Simulant run SB6-14 and SB8-A2 were the runs that were closest in acid stoichiometry and were included in this analysis. The data is summarized in Table 2-1.



**Table 2-1. Experiments and DWPF Batches Used in This Analysis**

Sludge Batch	SRAT Batch	Hsu Stoichiometry	REDOX Target
SB6	SB6-14	123%	0.20
SB6	SC-10	110%	0.20
SB6	535	115%	0.20
SB6	555	115%	0.10*
SB6	565	115%	0.10*
SB8	SB8-A2	131%	0.2
SB8	SC-14	133%	0.20
SB8	680	110%	0.146
SB8	705	115%	0.148
SB8	735	115%	0.151

\* Melter in bubbled operation with lower REDOX target

Requirements for performing reviews of technical reports and the extent of review are established in Manual E7 Procedure 2.60.<sup>43</sup> SRNL documents the extent and type of review using the SRNL Technical Report Design Checklist<sup>44</sup> contained in WSRC-IM-2002-00011.

### 3.0 Results and Discussion

A comparison will be made between Nitric-Formic Acid flowsheet processing in 4-L experiments with simulants, in 1-L experiments with actual waste, and in batch processing in DWPF. To limit the scope of this comparison, only three runs each from SB6<sup>22</sup> (runs 535, 555, and 565) and SB8<sup>29</sup> (680, 705, and 735) will be included, basically an early run (535), one in the middle of the sludge batch (565) and one near the end of the sludge batch (575). In addition, only the simulant and actual waste experiment with the acid stoichiometry closest to the DWPF acid stoichiometry will be discussed. This will make the comparison with processing conditions as close as possible.

This comparison will include key processing constraints (nitrite destruction and hydrogen generation), anion destruction, offgas chemistry, steam stripping and physical parameters (mixing, heat transfer, and foaming). Graphs and tables will allow comparison of the data at the three scales.

The purpose of the comparison is to demonstrate that DWPF Nitric-Formic Acid process flowsheets can be successfully developed by simulant testing and demonstrated using one actual waste experiment. Once DWPF has experience in processing a sludge batch at the acid stoichiometry recommended by SRNL (usually once ten batches have been completed), DWPF Engineering will adjust the acid stoichiometry within the operating window as needed to optimize processing.

Since the Nitric-Formic Acid flowsheet has been developed using this philosophy, it should be suitable for the Nitric-Glycolic Acid flowsheet also. The Nitric-Glycolic Acid flowsheet has a much more stable pH profile throughout processing and much lower hydrogen generation, both of which will make the process chemistry easier to predict and the flowsheet development much simpler. It is expected that the Nitric-Glycolic Acid flowsheet, the acid window, the target acid stoichiometry and the anion destruction data developed in simulant testing will be adequate for processing in DWPF. As is true with the Nitric-Formic Acid flowsheet, DWPF will be able to adjust targets as needed to optimize processing with the Nitric-Glycolic Acid flowsheet.

#### 3.1 Scaling Discussions

Scale-up from laboratory scale to full-scale can be a technical challenge. For some parameters such as reactor kinetics, the scaling is volumetric. For other parameters such as foaming, the scaling is based on the cross-section

area at the boiling surface. For parameters like internal reflux, headspace height is very important. As a result, flowsheet testing in equipment like the 1/216<sup>th</sup> scale SRAT may be ideal for reactor kinetics but is not conservative for foam testing due to the higher flux of the full-scale equipment.

In SRNL experiments, the scaling used was based on volume, trying to scale down from a 6,000-gallon sludge transfer to the appropriate volume in the laboratory SRAT vessel. As mixing is extremely important in ensuring optimum reaction kinetics, the mixing speed in experiments was chosen to visually provide good mixing by ensuring there is flow at the liquid surface and at the walls. If flow was seen at the surface and at the walls, the slurry was judged to be well mixed in the vessel as discussed in Section 3.7.1.

Many processing parameters are difficult to scale. An example of this is foaming. Two factors that are important to foaming are the gas flux at the boiling surface and the freeboard (height between liquid surface and top of vessel). It is impractical to have six feet of freeboard in an experiment with three liters of slurry (it will not fit in a hood). The gas flux is much lower in a small-scale experiment unless it is a very tall, narrow vessel. This too is impractical, as wall effects in a 1-inch diameter column would create more stable foam than in full-scale processing. Another example is steam stripping. In small-scale experiments, mercury vapor should be transferred with the gas to the condenser. Instead it may condense in the vapor space of the SRAT and not be collected in the Mercury Water Wash Tank (MWWT). If boilup time is important to understanding chemistry, design basis steam flow should be used, which may overestimate the mercury recovery. However, at the same time, the low gas flux at the liquid surface will limit the foam so the same test is not conservative for foaming. Table 3-1. lists the relative scale of the different scaled facilities compared to DWPF (a scale of one). Therefore, IDMS was a 1/5.36<sup>th</sup> scale vessel by volume but 1/1.75<sup>th</sup> by diameter. More scaling data can be found in Appendix C of SRNL-STI-2014-00306<sup>35</sup>, Revision 0.

**Table 3-1. SRAT and SME Relative Scaling\***

Parameter	DWPF	IDMS	1/216	22-L	4-L	1-L
Linear Nominal Height Scale (H)	1	1.75	6	11.0	20.9	28.3
Cross-Sectional Area Scale (A)	1	3.06	36	121.3	435	802
Vessel Volume Scale (H x A)	1	5.36	216	1,336	9,084	22,700
Vessel Nominal Contents Scale (from V <sub>L</sub> )	1	5.36	216	1411	7831	3
Total Volume (V <sub>T</sub> ), L	45,400 (12,000 gal)	7,570 (1,980 gal)	210 (55 gal)	22.0 (6 gal)	4.0 (1 gal)	1.4 (0.4 gal)
Nominal Contents Volume (V <sub>L</sub> ), L	22,700 (6000 gal)	4,230 (1120 gal)	105 (28 gal)	16.1 (4 gal)	2.9 (0.8 gal)	1.0 (0.3 gal)

\* Additional scaling information is included in Tables D-1 and D-2 in Appendix D

### 3.2 Process Window Chemistry

Since the composition of the sludge waste is different for each sludge batch, testing is needed to determine the process chemistry window for each sludge batch. A series of tests with simulants is used to determine the process chemistry window, between the upper and lower acid stoichiometry limits. The lower acid stoichiometry is determined by the minimum acid needed to destroy nitrite by the end of the SRAT cycle. The maximum stoichiometry is defined by the maximum acid where hydrogen generation does not exceed the SRAT hydrogen limit. A single test with actual waste is designed to demonstrate that the acid stoichiometry recommended (usually close to the low acid stoichiometry end of the operating window) leads to complete nitrite destruction and has hydrogen generation lower than the DWPF limit. An example of a sludge-batch operating window is shown in Figure 3-1.

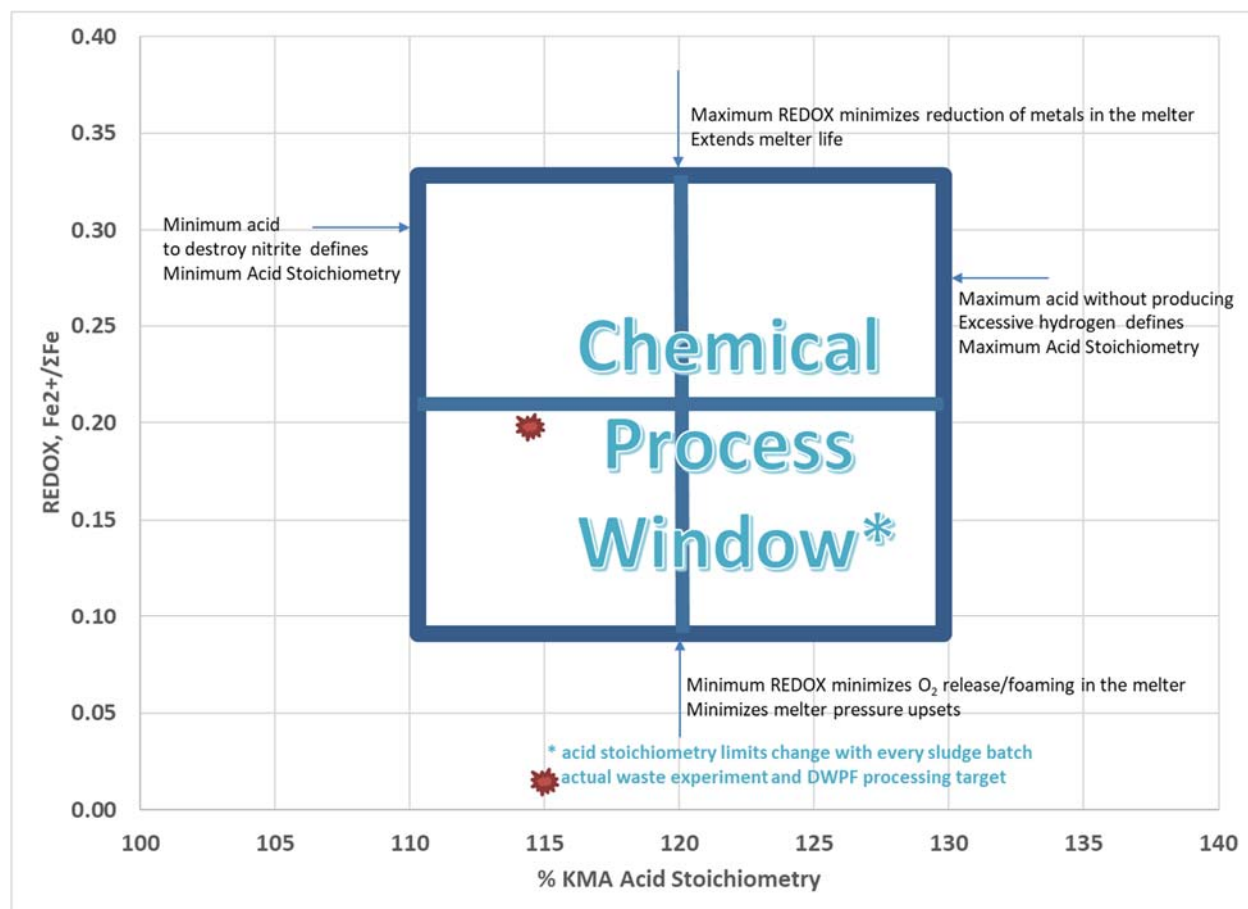
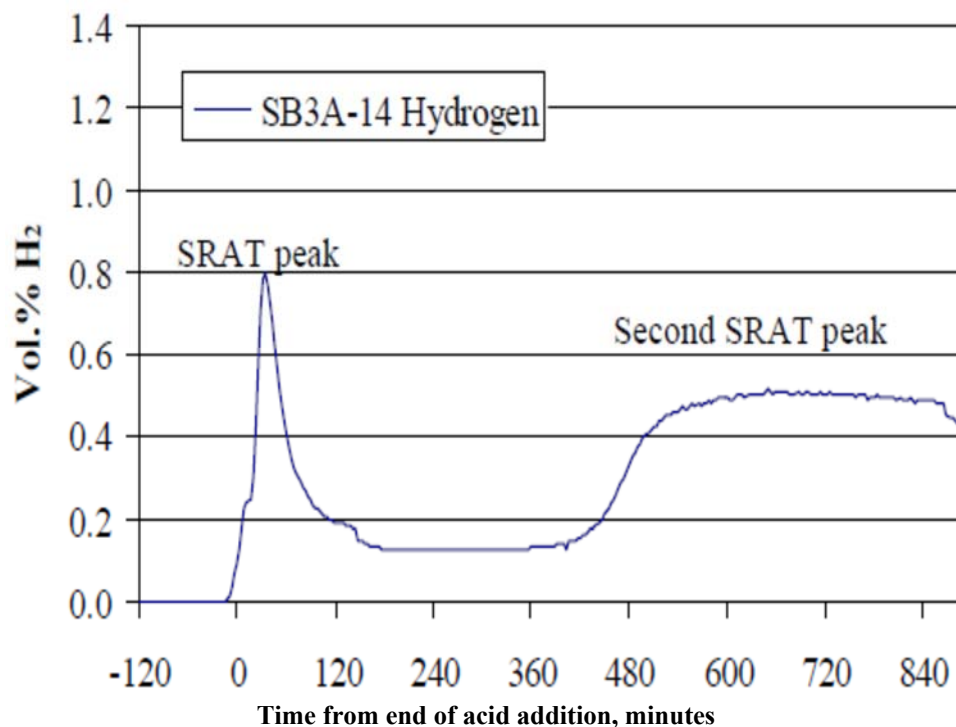


Figure 3-1. Example of a Sludge Batch Operating Window

### 3.2.1 Nitrite Destruction

The first key processing parameter in the Nitric-Formic Acid flowsheet is the destruction of nitrite. Nitrite forms a nitroso complex with rhodium, preventing the dehydrogenation of formic acid<sup>45</sup> to carbon dioxide and hydrogen. Once the catalyst is activated (maximum catalytic activity occurs after the nitrite is essentially destroyed), the generation of hydrogen can exceed the DWPF hydrogen generation limit if excessive acid is added. The peak hydrogen due to rhodium is generally the peak hydrogen for the run. However, the hydrogen concentration also decreases quickly (Figure 3-2). The second catalyst that generally becomes active after the rhodium has lost its activity is Ru. The second peak in Figure 3-2 is due to Ru. The hydrogen generation from Ru continues for days, so the Ru catalyst activity does not seem to change appreciably. Depending on the concentration and activity of the noble metals, in lower acid stoichiometry runs, the Rh peak will be lower, and the Ru peak can exceed the Rh peak.



**Figure 3-2. SRAT Hydrogen Generation Peaks Due to Rh and Ru**

Since the SRAT has a larger air purge than the SME, nitrite destruction followed by peak hydrogen generation in the SRAT is planned. However, in most experiments and in DWPF, the goal is demonstrated by the lack of nitrite in the SRAT product via an anion measurement. If the nitrite was not destroyed, inadequate acid was added during the batch. Table 3-2 summarizes the SRAT product nitrite concentration, demonstrating that nitrite destruction was complete in all batches chosen (except run 680 where the nitrite was 536 mg/kg, just above the detection limit of 513 mg/kg) for this report's comparisons (SB8 shaded in gray). The lower acid stoichiometry window is defined by the acid stoichiometry that does destroy the nitrite prior to the completion of the SRAT cycle.

**Table 3-2. SRAT Product Nitrite Concentration, mg/kg**

Sludge Batch	Run	Hsu Stoichiometry	Nitrite*
SB6	SB6-14	123%	<100
SB6	SC-10	110%	<1000
SB6	535	115%	<503
SB6	555	115%	<530
SB6	565	115%	<505
SB8	SB8-A2	131%	<500
SB8	SC-14	133%	<1300
SB8	680	110%	536
SB8	705	115%	<514
SB8	735	115%	<516

\* DWPF detection limits for nitrite may be higher than SRNL due to higher dilution levels

For nitrite destruction, in small scale testing with simulant and with actual waste and in typical DWPF processing, the nitrite was destroyed by the completion of the SRAT cycle.

### 3.2.2 Hydrogen Generation

The second key processing parameter in the Nitric-Formic Acid flowsheet is minimizing the hydrogen generation in the SRAT and SME. Hydrogen has a lower flammability limit of 4 volume % in air.<sup>46</sup> As was discussed above, the rhodium catalyst, tied up in a Nitroso complex, is not activated until the nitrite is destroyed. Destruction of nitrite in the SRAT typically results in the first hydrogen peak (often the biggest hydrogen peak) occurring in the SRAT cycle. The hydrogen generation limit prior to SB9 was 0.65 lb/hr in the SRAT cycle and 0.223 lb/hr in the SME cycle. In SB9, the hydrogen limit is 0.15 lb/hr in the SRAT and the SME cycle.

The scale-up calculation from the laboratory experiments to DWPF scale for any offgas measured during SRNL testing is defined by the following equation:

$$\frac{lb}{hr} \text{ in offgas} = V, \text{ vol \% gas} * He, \text{ sccm} * \frac{SL}{1000 \text{ sccm}} * \frac{60 \frac{min}{hr}}{\text{vol \% He}} * G \frac{g}{mol} * \frac{lb}{453.593 g} * \frac{mol}{24.146 L} * SF$$

$V$  = volume% of gas  
 $He$  = Helium purge, sccm  
 $\%He$  = volume % He  
 $G$  = g/mol of gas  
 $SL$  = Standard Liters  
 $SF = \text{Scale Factor} = \frac{6,000 \text{ gal DWPF sludge}}{\text{sludge volume, L}} * 3.785 \frac{L}{gal}$

In simulant testing, designed to determine the peak hydrogen generation predicted for DWPF, 125%<sup>†</sup> of the expected noble metal concentration is added to ensure the testing is conservative. In addition, the noble metals are added last prior to processing and are likely more active than the co-precipitated noble metals in actual waste.<sup>47</sup> In addition, a minimum purge is added, reflecting the minimum purge that will be applied in DWPF (factoring in the uncertainty in the purge flow). Lastly, no air inleakage is simulated to further increase the peak hydrogen concentration. As a result, the hydrogen generated in simulant experiments exceeds the hydrogen generated in shielded cells experiments and during processing in DWPF. The upper acid stoichiometry window is defined by the acid stoichiometry that does not exceed the hydrogen generation limit in the SRAT or SME.

The hydrogen concentration in SB6 processing is summarized in Figure 3-3 and Table 3-3. The hydrogen concentration in SB8 processing is summarized in Figure 3-4 and Table 3-3.

---

<sup>†</sup> Early sludge batch testing used a factor of 110%, but more recent tests have used 125%

Table 3-3. SRAT Hydrogen Peak Data for Nitric-Formic Acid Flowsheet

Sludge Batch	Run	Hydrogen, volume %	Hydrogen, lb/hr
SB6	SB6-14	0.118	0.087
SB6	SC-10	0.021	0.016
SB6	535	0.093	0.079
SB6	555	0.074	0.059
SB6	565	0.119	0.092
SB8	SB8-A2	0.161	0.174
SB8	SC-14	0.034	0.028
SB8	680	0.004	0.005
SB8	705	0.003	0.004
SB8	735	0.005	0.007

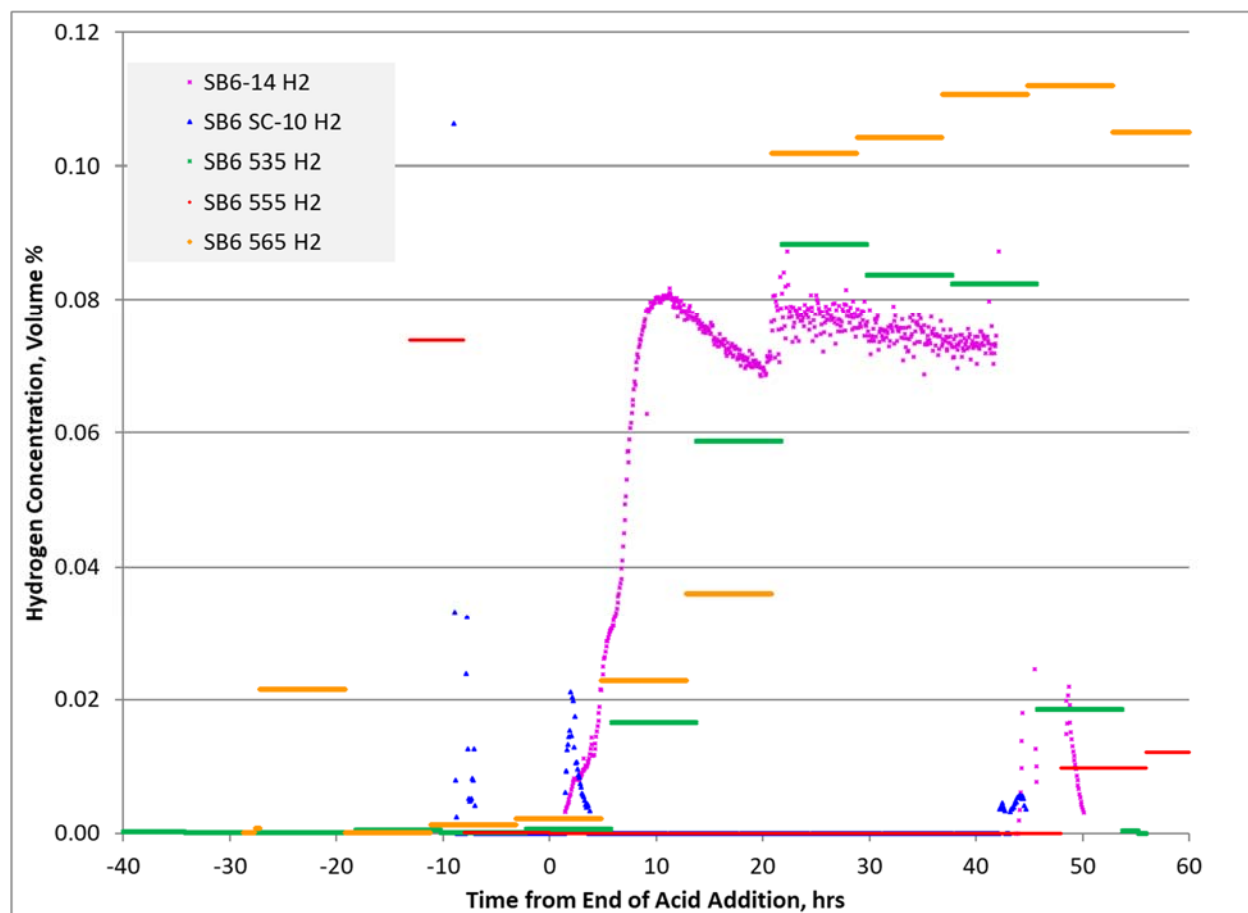
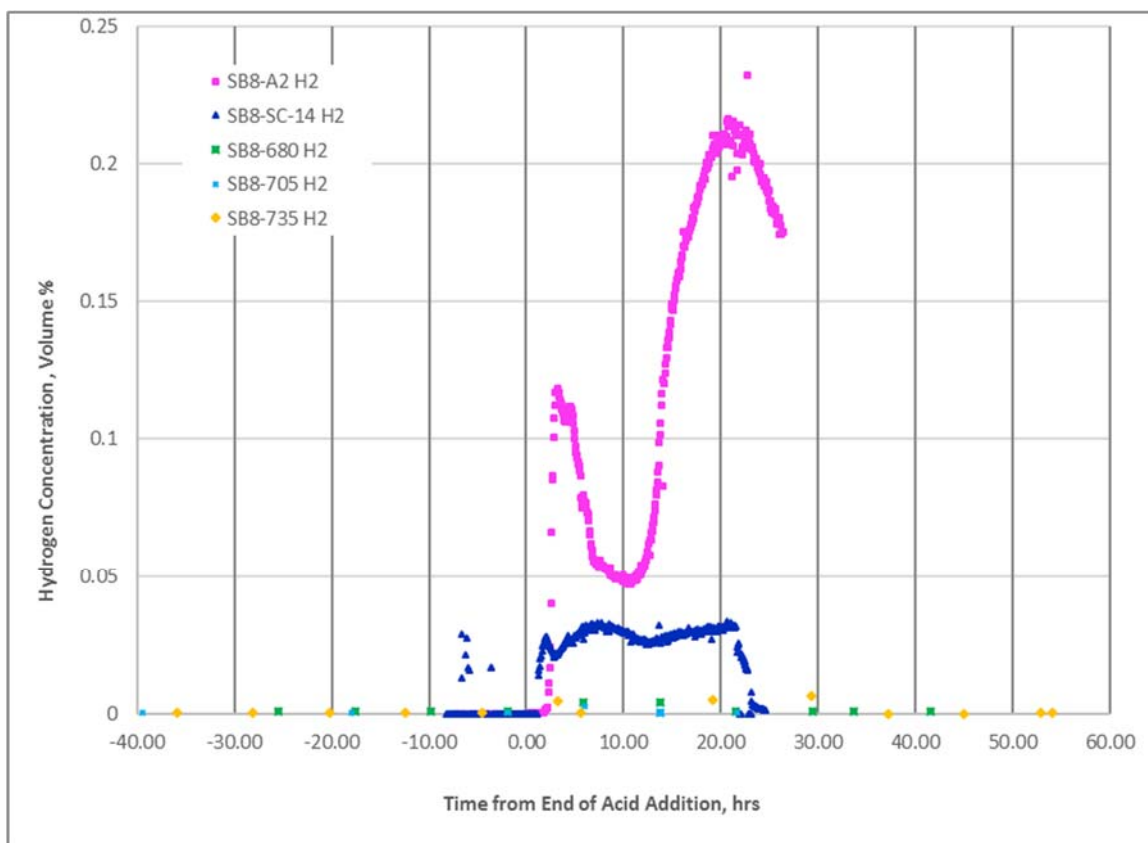


Figure 3-3. SB6 SRAT Hydrogen Concentration, Volume Percentage



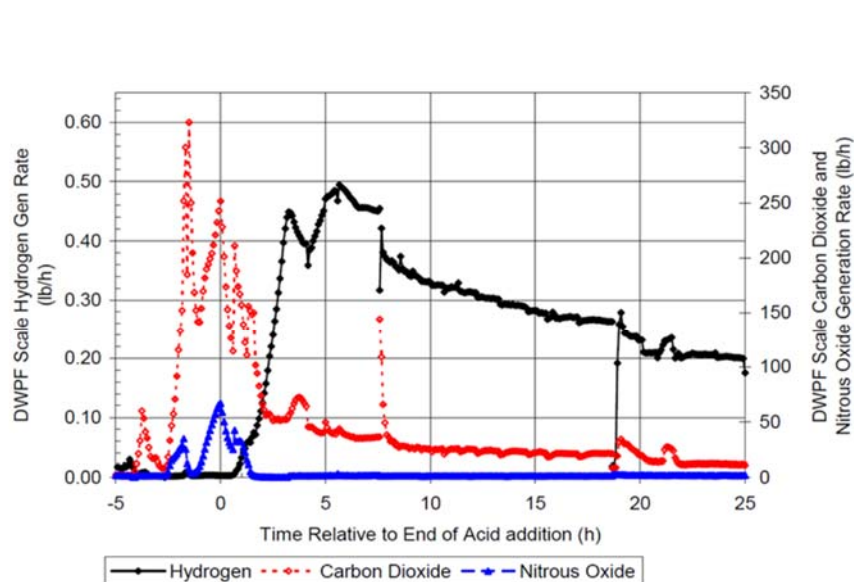
**Figure 3-4. SB8 SRAT Hydrogen Concentration, Volume Percentage**

As can be seen from the data above, the hydrogen was below the historical 0.65 lb/hr DWPF limits in all DWPF processing.

An evaluation of hydrogen generation using data collected by SRNL and DWPF Gas Chromatographs (GC) was completed by DWPF process engineer Brian Wingard in 2010. The results of this analysis were presented to SRR management in 2016<sup>48</sup>. The evaluation included a comparison of offgas profiles from SB5 shielded cells experiment SC-6 to DWPF Batch 474 (Figure 3-5). An evaluation was later made that compared maximum hydrogen generation from SRNL testing to DWPF processing for SB5, SB7a and SB8 (Table 3-4).

The SC-6 offgas profile for  $N_2O$  and  $CO_2$  is very similar suggesting the simulant was an acceptable surrogate for the actual waste. Hydrogen was significantly higher in the SRNL experiment than was seen in DWPF processing. This is consistent with the data comparison in Table 3-4 showing the hydrogen generation was significantly higher in SRNL experiments than in DWPF processing.

SRNL SRAT GC Data from SB5 Run SC-6



DWPF SRAT GC Data from SB5 Batch 474

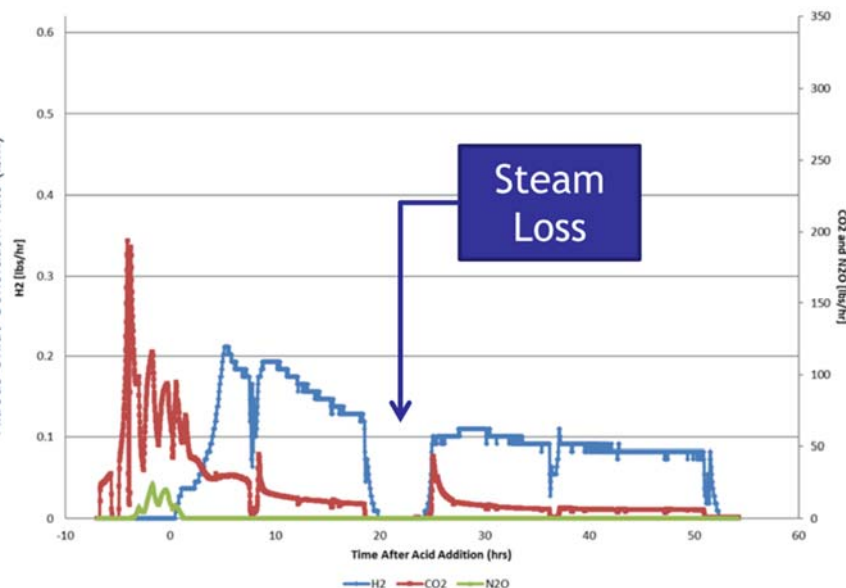
Figure 3-5. N<sub>2</sub>O, CO<sub>2</sub>, and H<sub>2</sub> profile from SRNL SC-6 and DWPF Batch 474

Table 3-4. Peak Catalytic Hydrogen Comparison Between SRNL and DWPF for the SRAT Cycle

	SB5	SB7a	SB8
SRNL Peak Hydrogen, lbs/hr	0.50	0.25	0.028
DWPF Peak Hydrogen, lbs/hr	0.23	0.018	0.0092

### 3.3 Anion Destruction

The SRAT receipt in DWPF contains nitrite, nitrate, free hydroxide, carbonate, aluminate, formate, phosphate, fluoride, and chloride. In SRNL experiments, the sludge simulant, without the added contribution of a heel, contains the above list of anions except it does not contain formate. Nitrate and formate are also added as nitric and formic acid during the SRAT process. Reduction of Mn and Hg oxidizes the formate to CO<sub>2</sub>(g). Noble metal catalyzed hydrogenation of formic acid also oxidizes the formic acid to CO<sub>2</sub>(g) and H<sub>2</sub>(g).



If the anion conversion ratios can be predicted, the anion concentration in the SRAT and SME products can be predicted. The anion conversion ratios are developed using simulant experiments and can be adjusted as needed in DWPF to produce a melter feed that achieves the REDOX target.

In DWPF, correction factors (CF) are used to calculate the final anion concentration. In SRNL, percent destruction or conversion is calculated. The equations used are described below:

$$CF = \text{Correction Factor} = \frac{\text{mols anion in product}}{\text{mols of anion in SRAT Receipt} + \text{mols of anion added with acid}}$$

$$\% \text{ Destruction} = 100\% - \frac{\text{mols anion in product}}{\text{mols of anion in SRAT Receipt} + \text{mols of anion added with acid}} * 100\%$$

$$\% \text{ Nitrite to nitrate Conversion} = \frac{(\text{Product nitrate} - \text{Receipt nitrate} - \text{acid nitrate}), \text{mols}}{\text{SRAT Receipt nitrite, mols}} * 100\%$$

### 3.3.1 Formate Destruction

In Nitric-Formic Acid flowsheet processing, the more acid that is added, the more formate is destroyed and the more carbon dioxide and hydrogen are generated due to noble metal catalyzed decomposition of formic acid. In addition, formate is destroyed due to the reduction of metals, primarily Hg and Mn. Table 3-5 summarizes the calculated percent loss and correction factors for formate.

In typical processing, approximately 20 to 30% of the formate is destroyed. This is affected by both the acid stoichiometry and the activity of the noble metal catalysts. In runs with higher acid stoichiometry and higher noble metal activity, the formate destruction will be higher.

The formate analysis has an analytical uncertainty of about 10% so the formate % loss has an uncertainty of 20%. Based on run SB8-A2, with a SRAT product formate concentration of 46,600 mg/kg, the formate destruction was 35.3%. If the formate concentration was 10% higher or 51,300, the formate destruction drops to 28.8%. If the formate destruction is low by 10% or 42,000 mg/kg, the formate destruction increases to 41.7%. The calculation of formate destruction uses three formate results, SRAT receipt formate, SRAT product formate, and formic acid addition, along with mass of each stream. The resulting variability can be even higher than this example demonstrates. Similar variability in formate destruction is seen in both DWPF processing and simulant experiments.

**Table 3-5. SRAT Formate Loss and Correction Factor Data**

Sludge Batch	Run	Hsu Acid Stoichiometry	Formate CF	Formate % Loss
SB6	SB6-14	120%	0.692	30.8
SB6	SC-10	110%	1.20	-19.6
SB6	535	115%	0.656	34.4
SB6	555	115%	0.829	17.1
SB6	565	115%	0.798	20.2
SB8	SB8-A2	131%	0.670	33.0
SB8	SC-14	133%	0.685	31.5
SB8	680	110%	0.587	41.3
SB8	705	115%	0.528	47.2
SB8	735	115%	0.599	40.1

Formate loss, in small scale testing with simulant and with actual waste, generally was within about 10% compared to typical DWPF processing. Formate loss is impacted by the concentration and activity of the noble metals along with processing time, which is different for simulant, actual waste and in DWPF. Because the formate loss was consistent in DWPF processing, it had little impact on REDOX.

### 3.3.2 Oxalate Destruction

Oxalate can be present in SRAT receipt samples, primarily due to oxalic acid cleaning of waste tanks and ARP crossflow filters. Oxalate is a difficult analysis, since the calcium and magnesium oxalate are insoluble. A special method for total oxalate was developed to improve quantification of oxalate but there is still considerable uncertainty in this measurement. For the SB6 runs, no oxalate was detected in the SRAT products, so this data was left out of Table 3-6. During SB6, the oxalate concentration in the feeds was low and the oxalate analysis was biased low.

In the Nitric-Formic Acid flowsheet, no oxalate is generated (in the Nitric-Glycolic Acid flowsheet, oxalate is produced in degrading the glycolic acid). Based on the SB8 results, some oxalate is destroyed. The oxalate percent destruction and correction factor were calculated for each SB8 batch and the results are summarized in Table 3-6.

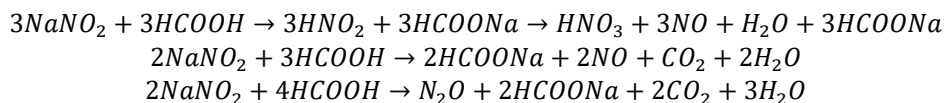
**Table 3-6. SB8 SRAT Oxalate Destruction and Correction Factor Data**

Sludge Batch	Run	Oxalate CF	Oxalate % Destruction
SB8	SB8-A2	0.680	32.2
SB8	SC-14	1.00	0.00
SB8	680	0.480	52.5
SB8	705	0.430	56.6
SB8	735	0.160	83.6

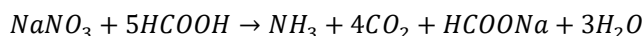
The oxalate loss varied considerably between small scale testing with simulant, and actual waste, and typical DWPF processing. Oxalate loss even varied within the three runs from DWPF that are included in the study. Although oxalate destruction varied, due to its relatively low concentration, it had little impact on REDOX.

### 3.3.3 Nitrite to Nitrate Conversion

During Nitric-Formic Acid flowsheet processing, the goal is to add enough acid to destroy the nitrite present in the SRAT. Nitrite reacts with acid through several paths to produce<sup>49</sup>:



In addition, the NO can be oxidized to NO<sub>2</sub> and the NO can be scrubbed as nitrite and nitric acid (nitrate). In high acid stoichiometry processing with active noble metal catalysts, the nitrate ion can be reduced to ammonia through the following reaction which consumes nitrate:<sup>49</sup>



In processing with high ammonia generation, the CF will be less than 1 and the nitrite to nitrate conversion will be less than zero due to reduction of nitrate to nitrite and nitrite to ammonia. The calculated nitrite to nitrate conversion and nitrate correction factor data is summarized in Table 3-7.

**Table 3-7. SRAT Nitrite to Nitrate Conversion and Nitrate Correction Factor Data**

Sludge Batch	Run	Nitrate CF	% Nitrite to Nitrate Conversion
SB6	SB6-14	0.942	-6.7%
SB6	SC-10	1.590	46.3%
SB6	535	1.124	14.4%
SB6	555	1.164	29.0%
SB6	565	1.195	32.8%
SB8	SB8-A2	1.10	11.10%
SB8	SC-14	1.49	43.60%
SB8	680	0.783	-35.50%
SB8	705	0.753	-34.20%
SB8	735	0.977	-3.20%

The nitrate and nitrite analyses both have an analytical uncertainty of about 10%. Based on run SB8-A2, with a nitrate concentration of 29,500 mg/kg, the nitrite to nitrate conversion was 11.1%. If the nitrate concentration was 10% higher or 32,500, the nitrite to nitrate conversion increases to 23.2%. If the nitrate analysis is low by 10% or 26,600 mg/kg, the nitrite to nitrate conversion decreases to -1.1%. The calculation of nitrite to nitrate conversion uses SRAT product nitrate, SRAT receipt nitrite and nitrate, and nitric acid addition, along with mass of each stream. Thus a 10% change in one or more of these inputs can easily change the % nitrite to nitrate conversion. Similar variability in nitrate destruction is seen in both DWPF processing and simulant experiments.

Two things should be pointed out in Table 3-7. First, the correction factor for nitrate (or the nitrite to nitrate conversion) is higher for the shielded cells runs. Two factors leading to higher internal reflux, which can affect conversion, are the large offgas volume and cool temperature in the vapor space of the kettle. These combine to scrub NO<sub>2</sub> in the SRAT vapor space and lead to higher nitrate concentration in the SRAT product. The larger (4-L) test rig used for simulant testing better matches the nitrate correction factor used in DWPF processing. Second, there is a lot of variability in this data.

The nitrite to nitrate conversion varied considerably between small scale testing with simulant, and actual waste, and typical DWPF processing, primarily due to the differences in internal reflux at the various scales. Nitrite to nitrate conversion is fairly consistent in DWPF processing. Because the nitrite to nitrate conversion was consistent in DWPF processing, it had little impact on REDOX.

### 3.4 Reduction/Oxidation (REDOX)

To produce glass that has a REDOX of 0.09 to 0.33, the proper blend of an oxidizing acid (nitric acid) and reducing acid (formic or glycolic acid) must be added during SRAT processing. The Jantzen REDOX equation is used to predict the REDOX of the glass.<sup>50</sup> In addition, the REDOX of the SME product (simulant or actual waste) is measured<sup>51</sup> in most experiments. Note that DWPF measures REDOX in glass approximately once per sludge batch using a pour stream sample so the measured REDOX results reported are from SRNL experiments.

$$\frac{Fe^{2+}}{\sum Fe} = 0.24 + 0.20 * (2F + 4C + 6G + 4O + 2.88 * C_A - 5N - ZMn) * 45 / T$$

F = formate (mol/kg feed)

C = coal (carbon) (mol/kg feed)

G = glycolate (mol/kg feed)

C<sub>A</sub> = carbon from antifoam, mol/kg feed

O = oxalate (soluble and insoluble) (mol/kg feed)

N = nitrate + nitrite (mol/kg feed)

Z = 0 for Nitric-Glycolic Acid flowsheet or 5 for Nitric-Formic Acid flowsheet

Mn = manganese (mol/kg feed)

T = Total Solids (wt %)

The predicted and measured composition of the SRAT products from some of the SB6 and SB8 runs is summarized in Table 3-8. The nitrite results were not included in the table since measured nitrite was less than detectable for most of the runs. The predicted results were corrected to the total solids measurement of the SRAT product sample.

**Table 3-8. Predicted and Measured Formate, Nitrate, Oxalate, and Mn for Predicting REDOX in SRAT Product Sample**

Sludge Batch	SB6					SB8				
SRAT Batch #	SB6-14	SC-10	535	555	565	SB8-2A	SC-14	680	705	735
Predicted Formate, mg/kg	45,300	42,900	43,300	45,900	43,300	75,181	63,445	37,006	37,303	33,032
Measured Formate, mg/kg	48,800	56,400	35,600	42,700	44,600	78,300	66,700	29,620	27,099	26,978
Predicted Nitrate, mg/kg	17,700	16,600	19,100	31,000	22,500	29,115	32,061	26,977	25,039	23,240
Measured Nitrate, mg/kg	18,500	18,600	16,800	28,500	28,000	29,550	37,900	17,540	15,791	18,835
Predicted Oxalate, mg/kg	0	50	0	0	101	4,020	NR	NR	NR	NR
Measured Oxalate, mg/kg	0	<100	<503	<507	<505	2,345	<130	1,686	1,056	1,508
Predicted Mn, wt % TS	5.23	4.04	4.21	3.53	4.22	7.57	8.09	4.65	5.14	4.94
Measured Mn, wt % TS	5.22	NR	3.97	3.14	3.47	7.26	5.73	2.29	2.63	2.47

NR is not requested

The SRNL acid calculation spreadsheet is used to predict the concentration of F, G, C, O, C<sub>A</sub>, Mn and T by mass balance and by estimating the destruction of F, G, O and N based on previous testing. A similar spreadsheet is used by DWPF. Both acid consumption and the REDOX model predictions can be used to calculate the REDOX target prior to the batch. The REDOX can also be predicted once the batch is complete using the measured concentration of these species, labeled in the table as Post SRAT REDOX Prediction. The input data and the predicted REDOX are summarized in Table 3-9.

**Table 3-9. Predicted SRAT Product REDOX at 36% Waste Loading**

Sludge Batch	SB6					SB8				
SRAT Batch #	SB6-14	SC-10	535	555	565	SB8-2A	SC-14	680	705	735
Hsu Acid Stoichiometry	123%	110%	115%	115%	115%	131%	133%	110%	115%	115%
Acid Ratio, Formic:Total	0.89	0.92	0.91	0.84	0.84	0.93	0.91	0.90	0.88	0.85
Formate (F), mol/kg	0.851	0.985	0.609	0.726	0.739	1.332	1.075	0.498	0.465	0.472
Oxalate (O), mol/kg	0.000	0.000	0.000	0.000	0.000	0.020	0.035	0.013	0.017	0.013
Nitrate (N), mol/kg	0.234	0.236	0.209	0.351	0.337	0.365	0.443	0.214	0.197	0.239
Mn, mol/kg	0.167	0.000	0.120	0.098	0.116	0.284	0.000	0.073	0.079	0.070
% Total Solids (T)	39	38.5	39.6	40.6	43.8	44.9	50.3	41.9	39.4	36.9
REDOX, $\text{Fe}^{2+}/\Sigma\text{Fe}$	SB6					SB8				
Acid calc Target	0.20	0.20	0.19	0.10	0.11	0.20	0.10	0.15	0.15	0.15
Post SRAT Prediction	0.17	0.42	0.15	0.07	0.08	-0.03	0.22	0.16	0.15	0.12

Predicted REDOX in small scale testing with simulant and with actual waste, generally was within about 0.05 compared to typical DWPF processing. Predicted REDOX is impacted by formate, oxalate, and nitrate concentration. Despite the variability of these anions, it had little impact on REDOX.

### 3.5 Mercury Stripping

Mercury removal in DWPF is designed to remove elemental mercury from the SRAT and SME slurry and collect the mercury in the MWWT or Slurry Mix Evaporator Condensate Tank (SMECT). A series of steps is involved including (1) the reduction of mercury in the feed to elemental mercury, (2) steam stripping of the mercury from the SRAT or SME, (3) condensation of the mercury in the SRAT or SME condenser, ammonia scrubber or FAVC, (4) coalescence of the mercury, and (5) collection of the mercury in the MWWT or SMECT. In theory, it takes 250 lb steam per lb elemental mercury at boiling conditions in the SRAT or SME. In practice, it takes more than 750 lb steam per lb of elemental mercury. In both SB6 and SB8, the time at boiling was calculated to remove enough mercury to meet the 0.45 wt % mercury target assuming it takes 750 lb steam per lb of mercury. For a SRAT product, the Hg concentration should be  $\leq 900$  mg/kg at 20 wt % total solids or  $\leq 1125$  mg/kg at 25 wt % total solids. The SRAT product mercury data is summarized in Table 3-10.

In SB6, the mercury stripping efficiency in DWPF was poor based on the mercury concentration in the SRAT product. During SB6, the SRAT mercury endpoint target was raised from 0.45 to 0.60<sup>52</sup> to 0.80 wt % because of the inefficient mercury stripping and to shorten processing time. Because mercury continues to be stripped in the SME cycle, the SRAT cycle stripping time was shortened and credit was given for the mercury stripped in the SME cycle to meet the 0.45 wt % mercury target.<sup>52-53</sup> Based on sample results from batches 531-569, the average SRAT Receipt mercury concentration was 3,583 mg/kg, the average SRAT product mercury concentration was 1,943 mg/kg, the maximum SRAT product concentration was 3,379 mg/kg, and the average total solids was 22.3 wt %. The mercury concentration should have been  $\leq 1,005$  mg/kg to meet the 0.45 wt % target.

In SB8, the mercury stripping efficiency in DWPF was better than SB6. Based on sample results from batches 671-681, the average SRAT Receipt mercury concentration was 2,181 mg/kg, the average SRAT product mercury concentration was 738 mg/kg or 0.27 wt %, the maximum SRAT product concentration was 1,610 mg/kg or 0.45 wt %, and the average total solids was 22.7 wt %. The average mercury concentration was below the target of  $\leq 0.45$  wt %.

**Table 3-10. SRAT Product Mercury Data**

Sludge Batch	Run	Mercury, mg/kg	Mercury, Wt % total solids basis
SB6	SB6-14	1,025	0.46
SB6	SC-10	414	0.19
SB6	535	887	0.41
SB6	555	2,568	1.15
SB6	565	2,869	1.16
SB8	SB8-A2	2,155	0.77
SB8	SC-14	2,238	0.71
SB8	680	541	0.23
SB8	705	NR	NA
SB8	735	NR	NA

Recent testing with the Nitric-Glycolic Acid flowsheet suggests that mercury stripping is more efficient at higher boilup rates.<sup>38</sup> Efficient steam stripping requires excellent mixing with no holdup of mercury at the bottom of the vessel or hiding in corners. Any mercury not measured in the sample is assumed to have been steam stripped in the above analysis. As a result, the mercury stripping efficiency could be even lower than estimated in Table 3-10 for experiments with simulants as elemental mercury is often found “hiding” in the SRAT. In actual waste experiments and DWPF, there appears to be no accumulation of mercury in the SRAT, so the SRAT product results can be used to predict mercury removal.<sup>54</sup>

Recent analysis of samples from DWPF have demonstrated that the mercury fed to the SRAT is a combination of mercury oxide, elemental mercury and organic mercury (primarily methyl mercury).<sup>55</sup> In addition, mercury can be dissolved in the acidic condensate produced during SRAT processing. To date, Tank 40 or SRAT samples have not been analyzed to determine the split of mercury species in the SRAT.

**Recommendation:** Complete future flowsheet development testing at the scaled boilup rate that DWPF plans to use. Testing at plant operating conditions, not design basis, should be the condition for most testing, as design basis does not simulate the time at temperature or mercury stripping in DWPF processing. Since the mercury collection and the various mercury forms in the condensate will depend on the speciation of the sludge, ARP and SEFT, the mercury added to simulants should reflect this when the objective is to better understand mercury stripping and collection in the MWWT.

### 3.6 Offgas Chemistry

In laboratory experiments, a minimum purge is specified that reflects the lower bound air purge instrument uncertainty. The offgas includes the SRAT air purge (230 scfm in experiments and approximately 265 scfm in DWPF), air inleakage (zero in experiments due to a small positive pressure, unknown in DWPF due to processing under vacuum), and any gasses generated or consumed during processing. In experiments, the gas generation can be calculated from the helium tracer and in DWPF it can be estimated from the nitrogen concentration. The offgas profiles throughout the SRAT cycles will be compared to determine how consistent they are for both SB6 and SB8. Data from simulant and actual waste experiments will be compared to data collected during DWPF processing. Due to the higher purge in DWPF and the air inleakage, the peak heights for offgas species will be significantly lower than for experiments even if the scaled offgas generation rates are the same. Additional offgas data is included in Appendix B.

Note also that the simulant and actual waste for experiments is prepared months before the actual waste is ready in Tank 40. As a result, the concentrations of nitrite and carbonate may be slightly different in experiments compared to DWPF. In addition, pump seal inleakage of inhibited water will slowly dilute the waste in Tank 40, so the anion concentration will be lower in later DWPF processing than in earlier processing and a lower concentration of noble metals will be present in each 6,000-gallon sludge addition to DWPF. If the dilution in Tank 40 is excessive, Tank 40 may be decanted to restore the concentration or caustic boiling will be used together with making a third addition of sludge to prepare the batch. The result of these changes mentioned above is that when comparing experiments to DWPF processing, the offgas profile will be different.

Reaction kinetics is often impacted by acid stoichiometry. Therefore, any error in sludge composition or volume will lead to an error in acid addition. If more acid is added due to these errors, the offgas peaks will be sharper and will end sooner. Therefore, although the runs that were compared were chosen to have approximately the same acid stoichiometry, the actual offgas profile might look different due to errors in the calculated acid leading to the addition of more acid.

Reaction kinetics is often strongly impacted by catalyst concentration and activity. For example, in SB9 simulant testing, the rhodium concentration target was 0.0156 wt percentage on a total solids basis or 24.4 mg/kg. This was added at 125% of the measured concentration to be conservative because of the relatively high uncertainty of the noble metal analytical result. In simulant testing, fresh noble metal is added, which is more active than the same concentration of noble metal in actual waste. The freshly added noble metal is more likely to be on the surface of sludge particles, not imbedded in a co-precipitated particle. The result is that in simulant experiments the kinetics may be faster leading to sharper peaks and may lead to shorter reaction times. This is done intentionally in each sludge batch flowsheet development to minimize the risk of higher reaction rates and higher hydrogen concentrations during DWPF processing than in the simulant tests. Again, the result is that the offgas profiles might look different.

Although DWPF has two GC columns, only the column that measures hydrogen is currently operable. The column that measures CO<sub>2</sub> and N<sub>2</sub>O has been inoperable since the middle of SB6 so little data is available from DWPF processing. As a result, the nitrogen profile and oxygen profile will be discussed as they infer the presence of gases that are not being measured. For example, if NO is oxidized to NO<sub>2</sub>, the oxygen concentration will decrease more than the nitrogen concentration. If both oxygen and nitrogen are diluted by the same fraction, no oxygen is being consumed, if both nitrogen and oxygen decrease by the same fraction, the dilution is caused by the generation of reaction decomposition products. So primarily, the data collected from the operable DWPF columns (H<sub>2</sub>, N<sub>2</sub>, O<sub>2</sub>) will be discussed.

### 3.6.1 Offgas Species

The offgas flow contribution for each offgas component at DWPF can be calculated from the air purge plus air inleakage and the offgas concentration. Since the air inleakage is not measured, it was assumed to be zero in the calculations below, meaning the calculation could be underestimating the offgas flows. Nitrogen is inert in CPC processing, so the concentration of nitrogen can be used to determine the offgas flow. The total offgas flow is calculated as follows:

$$\text{Offgas Flow, scfm} = \text{SRAT Purge Flow, scfm} * 78.09 / N_2$$

The contribution from each offgas species can be calculated knowing the offgas flow and GC measured gas concentration. In addition, the concentration of other gases not measured (primarily argon) can be estimated using the ratio of these other gases to nitrogen in air (78.09% N<sub>2</sub>, 20.95% O<sub>2</sub>, 0.98% other, primarily argon and CO<sub>2</sub>). A graph showing the calculated flowrate for each gas is summarized in Figure 3-6. Note that nitrogen is plotted on the right y-axis and its scale is 3.73 times the left y-axis scale as the nitrogen concentration in air is 3.73 times that of oxygen. The flowrate of nitrogen is constant throughout processing at about 205 scfm. If no oxygen is being consumed, the oxygen line should be on top of nitrogen line, as it is until about 1 hour before the end of acid

addition and is again from about the 3-hour mark after acid addition and throughout the rest of the SRAT cycle. During periods where no oxygen is being consumed, its flow is about 55 scfm.

The oxygen depletion will be discussed in Section 3.6.2 and the contribution from NO oxidation will be discussed in Section 3.6.3. Note also that the nitrogen flowrate drops during the latter part of acid addition and early part of boiling due to the smaller vacuum in the SRAT vapor space and lower air inleakage during periods of high gas generation of carbon dioxide and oxides of nitrogen.

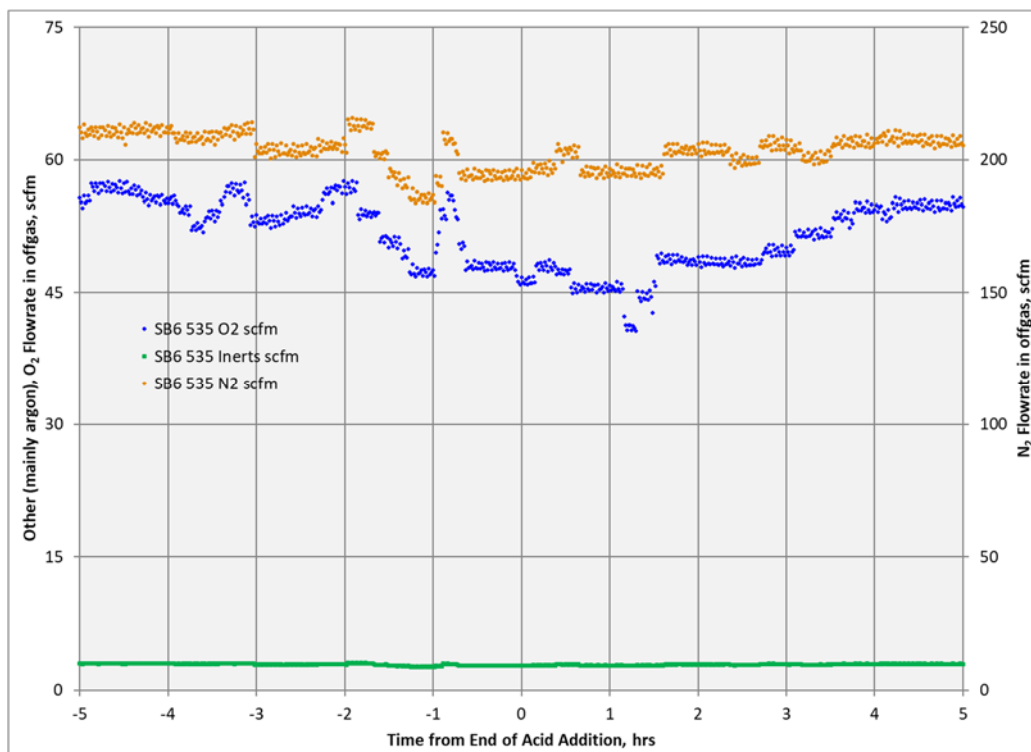


**Figure 3-6. Calculated Offgas Flowrates, scfm for DWPF Batch 535**

### 3.6.2 Oxygen Depletion and Nitrogen/Oxygen Ratio

Oxygen is consumed in several reactions, included oxidizing NO to NO<sub>2</sub>. This occurs in all runs for all sludge batches. It is shown graphically in the SB6 and SB8 oxygen graphs (Figure 3-7 and Figure 3-8). Note also that the oxygen drops to a lower concentration in the simulant runs than in DWPF due to DWPF's larger air purge. The oxygen drop in SB6 is smaller than the oxygen drop in SB8. The oxygen depletion can be calculated as follows:

$$O_2 \text{ Depletion, scfm} = N_2 \text{ flowrate, scfm} / 3.73 - O_2 \text{ flowrate, scfm}$$

The depletion is shown graphically in Figure 3-9.



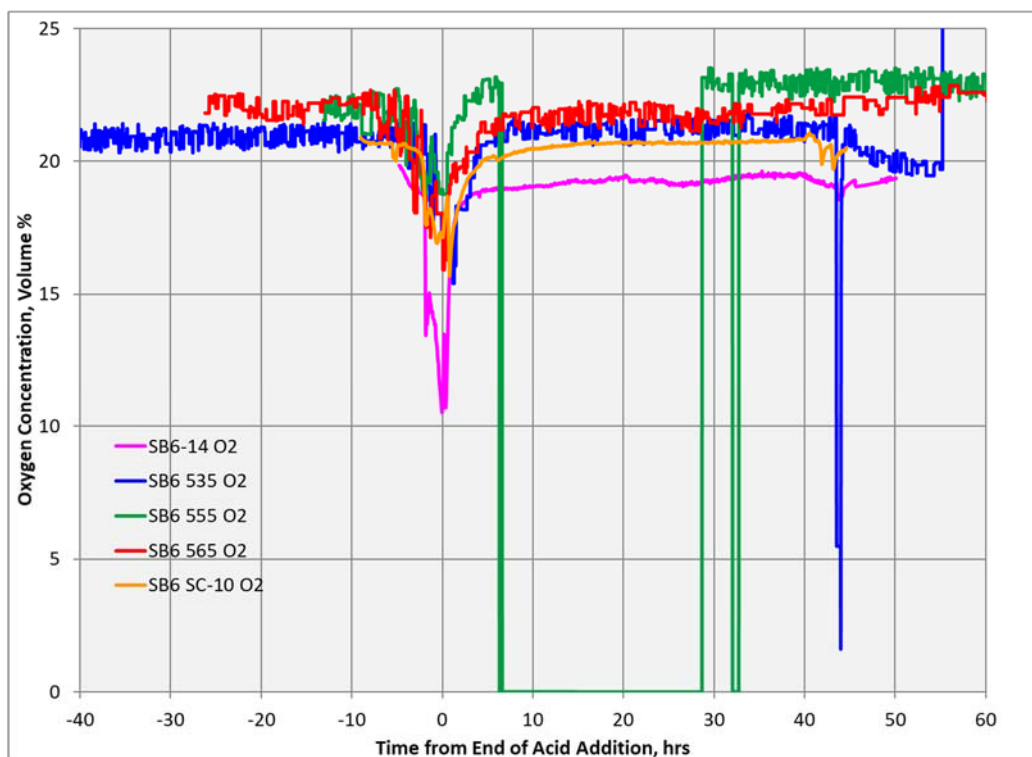


Figure 3-7. Oxygen Profile for Selected SB6 Experiments and DWPF Batches

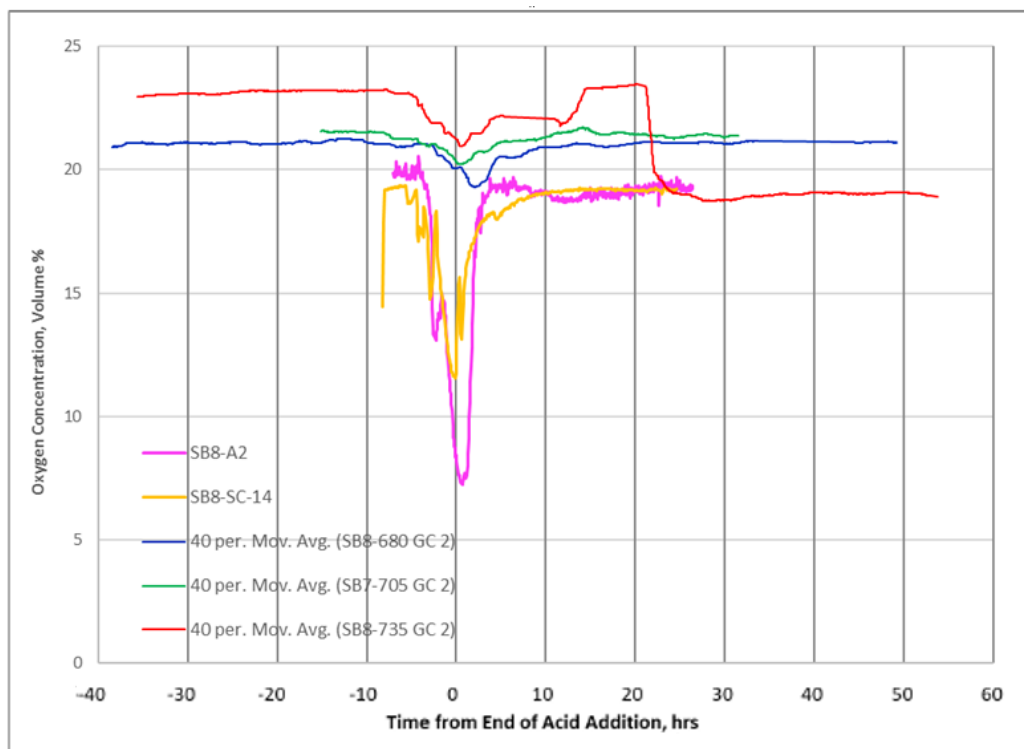
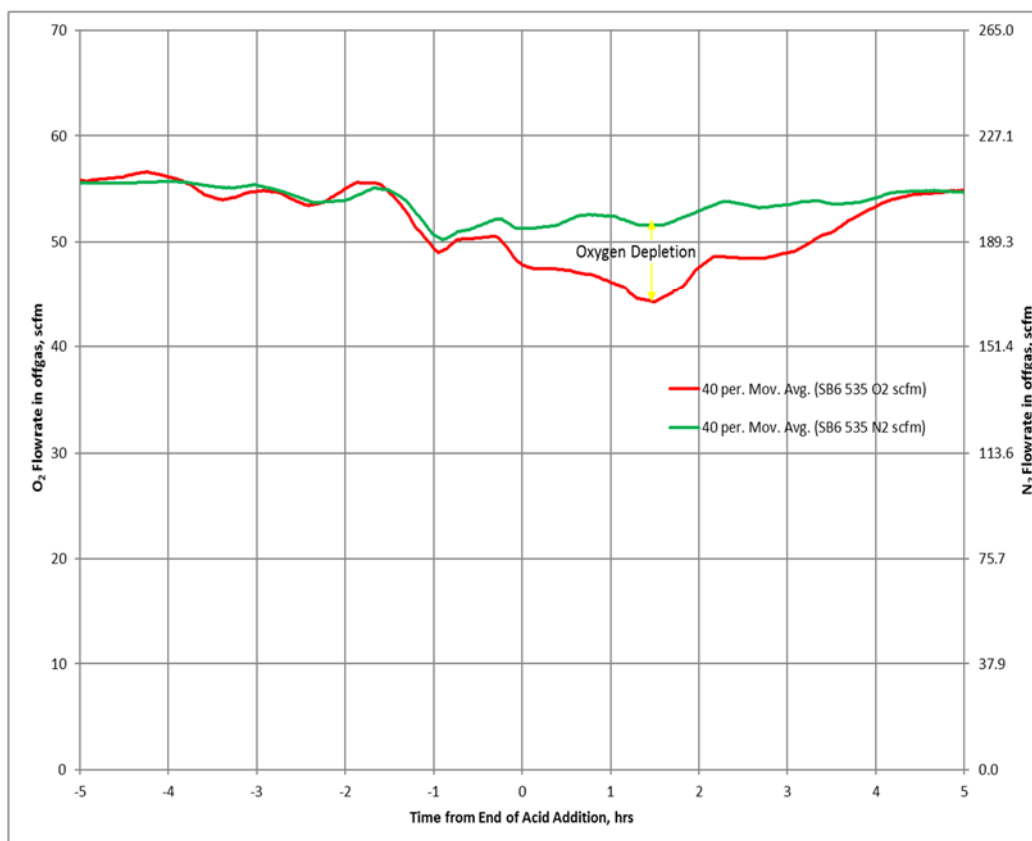


Figure 3-8. Oxygen Profile for Selected SB8 Experiments and DWPF Batches



**Figure 3-9. SB6 535 Oxygen Depletion, Nitrogen and Oxygen Offgas Flow, scfm**

The oxygen profile and the depletion of oxygen during processing followed the same trend in simulant experiments, experiments with actual waste and DWPF processing.

### 3.6.3 Oxides of Nitrogen Generation

Nitrite is destroyed through several paths, producing  $\text{N}_2\text{O}$ , NO and  $\text{NO}_2$  in the offgas. The NO can be oxidized to  $\text{NO}_2$ . The  $\text{NO}_2$  can be scrubbed in the SRAT vapor space (internal reflux), SRAT condenser, SRAT Scrubber or Formic Acid Vent Condenser (FAVC), producing nitric and nitrous acid in the SRAT liquid or SMECT liquid.

In most Nitric-Formic Acid flowsheet experiments completed to date, the use of GCs allowed the measurement of only  $\text{N}_2\text{O}$ . In more recent experiments, the addition of a mass spectrometer and Fourier Transform Infrared spectrometer (FTIR) allows the measurement of  $\text{NO}_2$ , NO, and  $\text{N}_2\text{O}$ . The measurement of the oxides of nitrogen is complicated by the fact that the NO can be oxidized to  $\text{NO}_2$  in the SRAT offgas and the  $\text{NO}_2$  can be scrubbed in the SRAT vapor space, the SRAT condenser, the ammonia scrubber, and the FAVC. The offgas in experiments and DWPF is pulled after the FAVC. This means that most of the  $\text{NO}_2$  is scrubbed out (into the SRAT slurry and condensate) so the measured concentration of NO and  $\text{NO}_2$  is typically much less than would have been measured in the SRAT vapor space.

Since DWPF has not used the GC to measure  $\text{N}_2\text{O}$  since the beginning of SB6, calculations will be used to determine the generation of offgas species using the depletion of oxygen. This methodology assumes that nitrite decomposes to NO, is oxidized to  $\text{NO}_2$  in the vapor space, and the only oxygen consuming reaction is the oxidation of NO.

### 3.6.4 Carbon Dioxide Generation

Carbon dioxide is generated from the destruction of carbonates during acidification of the sludge and the consumption of formic acid during the reduction of Mn and Hg. The added acids will bring the pH down to approximately 5.5, when a large carbon dioxide peak is generated due to carbonate destruction. The concentration of the CO<sub>2</sub> peak is controlled by slowly metering in the acids. No comparison with CO<sub>2</sub> can be made with DWPF since the GC's B column, used to measure N<sub>2</sub>O and CO<sub>2</sub>, was not in service during SB6 or SB8.

## 3.7 Physical Parameters Important to Processing

To simplify the data analysis, only mixing, heat transfer and foaming will be discussed.

### 3.7.1 Mixing and Heat Transfer

Mixing was extensively studied prior to the design and construction of DWPF. The agitation system (impeller speed, diameter, and design) was specified by the Ekato Method as described in a 2004 Marinik/Stone report.<sup>56</sup> A relationship between mixing speed and vessel diameter was developed as summarized in Figure 3-10. This relationship was developed using testing at two different scales using a physical simulant. A thorough summary of the mixing calculations is included in Appendix D.

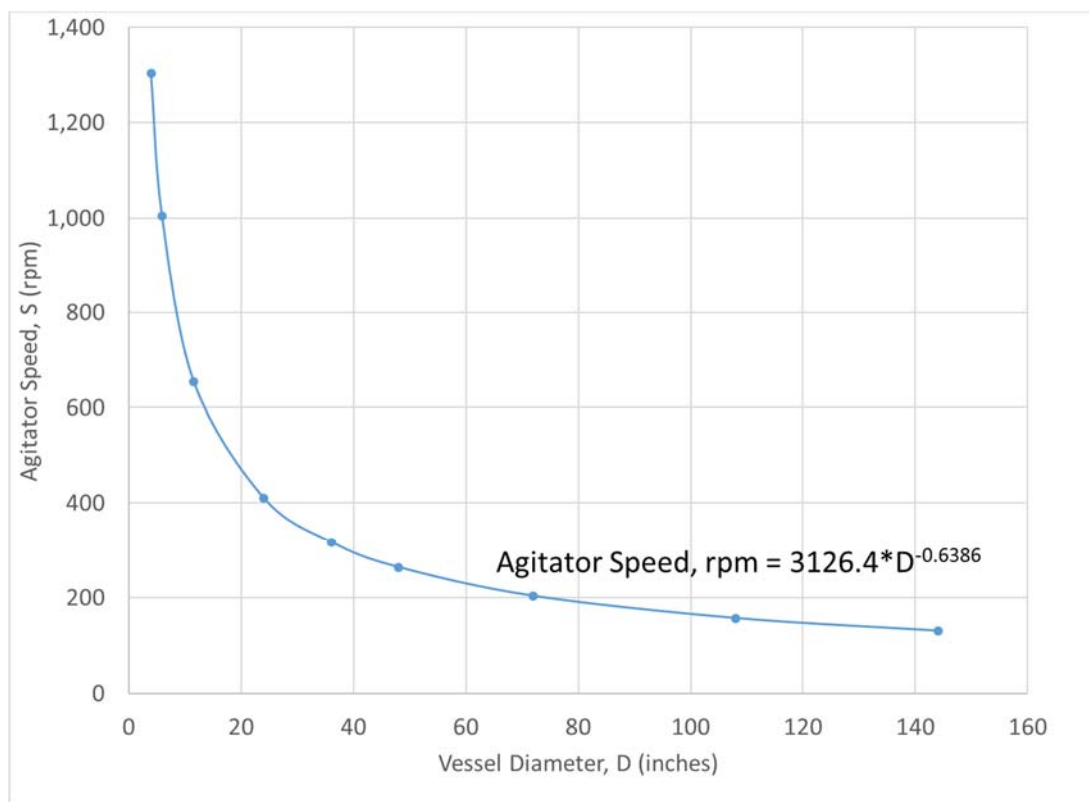


**Figure 3-10. Ekato Method for Predicting Mixing Speed at Different Scale**

The Marinik/Stone report discussed six methods for scaling down from full-scale to the experiments. Each of these methods will calculate a different mixing speed as vessel diameter decreases due to differences in these methods. These calculations are complicated by the fact that the actual waste behaves like a Bingham plastic fluid whose rheology changes both from one sludge batch to another and throughout SRAT processing. In addition, not only is the rheology changing but also the volume changes throughout batch processing. So, in experiments, calculations

can be made to scale down to target an approximate agitation rate, but the needed agitation speed is determined visually by the researcher to ensure “good mixing”, defined as mixing at the liquid surface and walls without an excessive vortex. The agitation rate often is adjusted during testing due to the thinning of the slurry by acid addition and the lower volume that needs to be mixed after dewatering is complete.

In recent years, the experimental rigs have been improved to add sensors needed for calculating the heating rod heat transfer coefficient (a measure of heat transfer). The heat transfer coefficient also is a good predictor of mixing. If mixing is adequate and there is no fouling of the heat exchange surface, the heat transfer at constant temperature should also be constant.

For effective heat transfer, mixing should sufficiently blend miscible liquids so that the “hot” fluid near the heated surface is dispersed throughout the vessel and replaced by “cooler” fluid. If the fluid in the vessel is a Bingham plastic, the mixing cavern should cover the entire working volume of the vessel.

Heat transfer efficiency can be calculated using the following equation<sup>57</sup>:

$$Q = UA\Delta T$$

Q= heat input from steam, W

A=Heat transfer area, cm<sup>2</sup>

$\Delta T$  = Temperature difference between steam and boiling liquid in SRAT, °C

U=Heat Transfer Coefficient, W/cm<sup>2</sup>/°C (IDMS design basis was 0.064 W/cm<sup>2</sup>/°C)

Unless the heat exchanger surface fouls, it is expected that the heat transfer coefficient is constant throughout boiling although it may drop a little during evaporation.

The SRAT heat transfer coefficients during the 535 and 565 SB6 batches in DWPF are plotted in Figure 3-11. This shows a significant increase in the heat transfer coefficient from about 0.050 to about 0.065 W/cm<sup>2</sup>/°C between these batches. Figure 3-12 is a graph showing the heat transfer coefficients during DWPF SB8 batches 680 and 735. This shows the heat transfer coefficient has dropped to about 0.045 W/cm<sup>2</sup>/°C. These figures show that during the boiling phase, the heat transfer coefficient is relatively constant for a given batch.

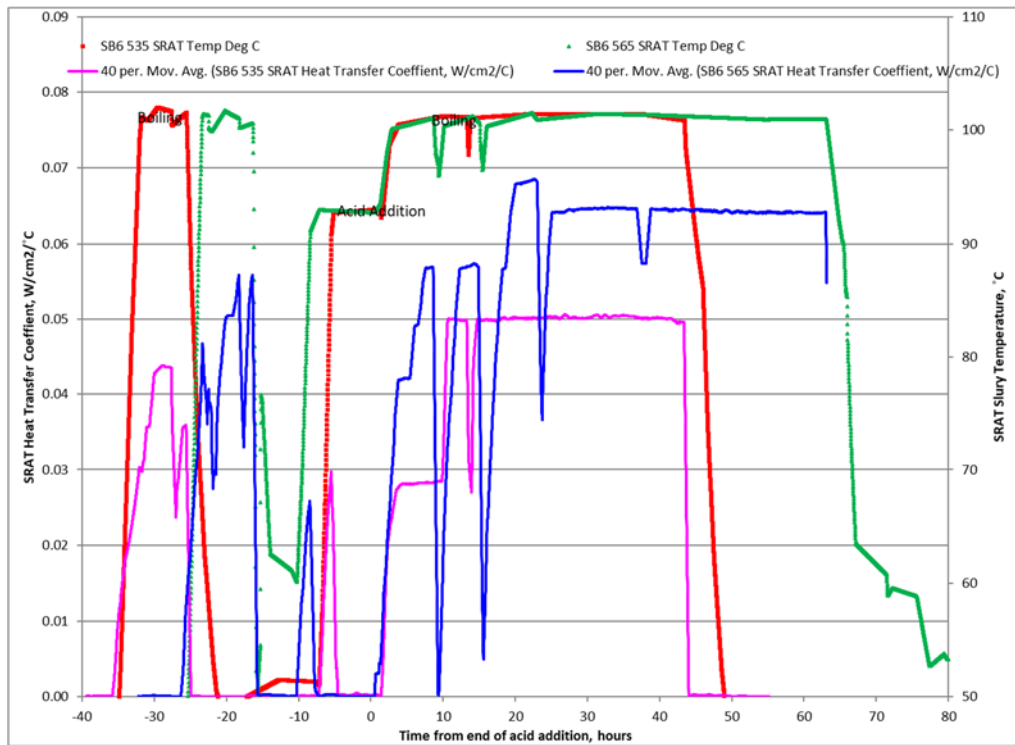


Figure 3-11. SB6 Calculated Heat Transfer Coefficient for DWPF SRAT Steam Coils

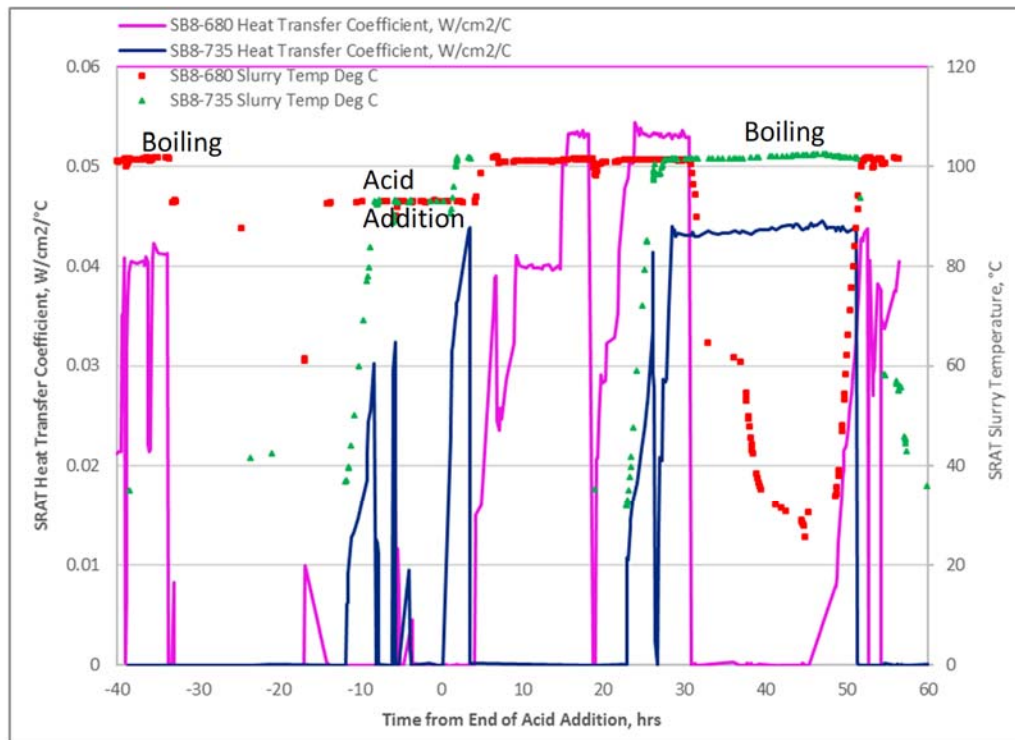
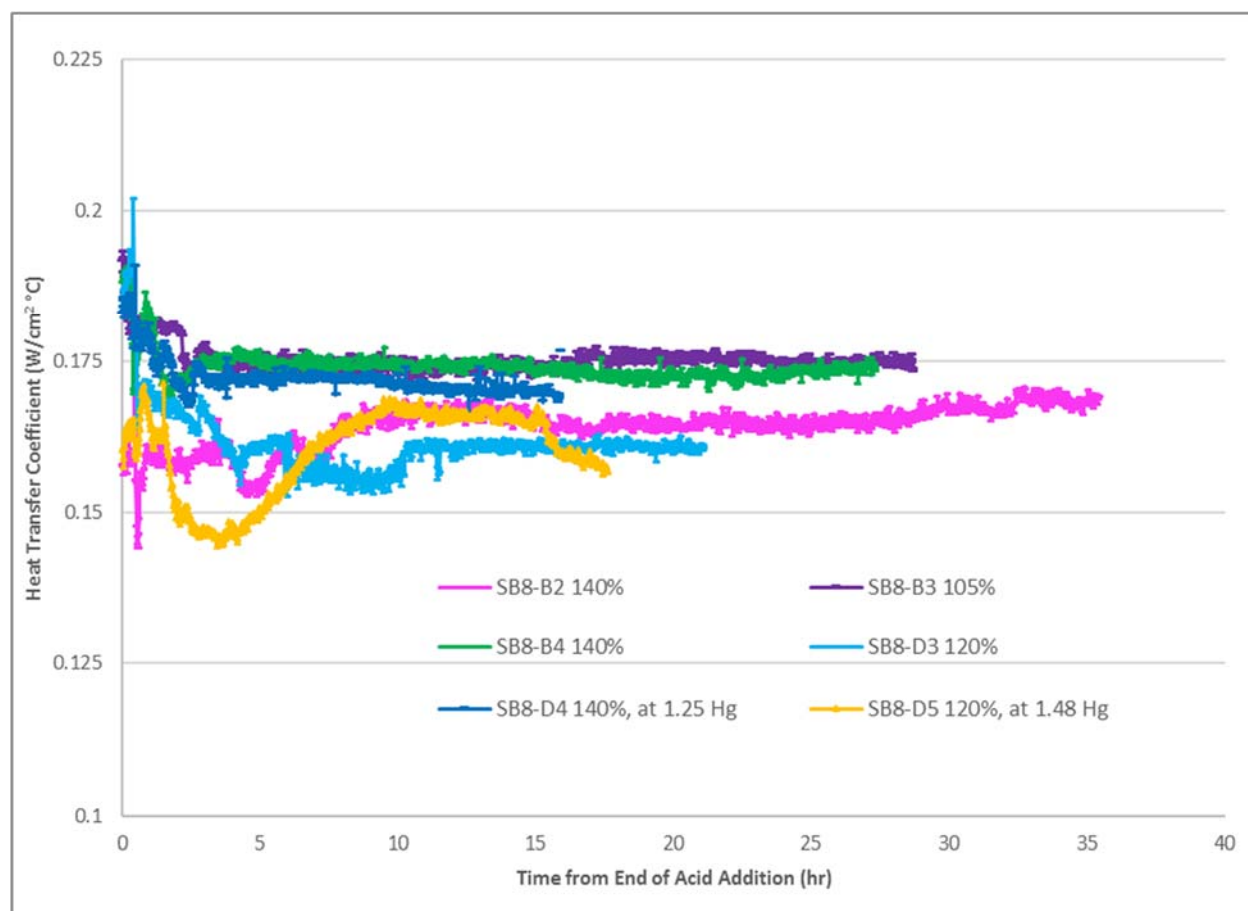


Figure 3-12. SB8 Calculated Heat Transfer Coefficient for DWPF SRAT Steam Coils

The equipment used for simulant testing was modified between SB6 and SB8 to change the heating source from a mantle to heating rods. The heating rod thermocouples allow a calculation of  $\Delta T$ . In addition, the power to the rods is continually measured so the heat transfer coefficient can be calculated. The calculated heat transfer coefficients varied from about 0.15-0.20 W/cm<sup>2</sup>/°C, as shown in Figure 3-13.

The difference between the heat transfer coefficients between the DWPF and simulant laboratory testing is most likely due to the different regime of flow that is occurring in the process. Based on the mixer Reynolds numbers, the laboratory testing is in laminar or transitional flow whereas the DWPF process is in turbulent flow. The heat transfer coefficient between DWPF and IDMS are similar, and both processes are turbulent.



**Figure 3-13. SB8 Laboratory Scale Calculated Heat Transfer Coefficient for Heating Rods**

Mixing is influenced by the rheological properties of the slurry. In designing equipment where mixing is an essential component, the simulant would have to be adjusted to replicate the key rheological properties versus the chemistry as has been done for flowsheet development. For defining the chemistry, visibly ensuring mixing as has been described here has been demonstrated to provide chemistry that replicates DWPF operation.

### 3.7.2 Foam/Antifoam

Antifoam has been added to the SRAT and SME since startup due to the foaming tendency of the SRAT and SME materials caused by offgas generation of NO, NO<sub>2</sub>, N<sub>2</sub>O, and CO<sub>2</sub>, and the generation of water vapor during boiling. Since 1999, Antifoam 747 has been added as an antifoam and defoamer. The antifoam is most stable at a neutral pH and degrades faster as the pH deviates from neutral.<sup>58</sup> The antifoam begins degrading upon dilution with water (historically, a five wt % solution of antifoam was utilized at DWPF) and degrades more rapidly after being added to the SRAT or SME due to the higher temperature and non-neutral pH.

Throughout SB6 runs, diluted antifoam was prepared and added as needed. During SB9 runs, undiluted antifoam was added followed by a water flush. The antifoam addition strategy for SB6 and SB8 is summarized in Table 3-11. Degradation products formed during storage of the diluted antifoam and during processing are volatile at SRAT and SME processing conditions and lead to high concentrations of flammable antifoam degradation products immediately after the diluted antifoam is added. To reduce this antifoam degradation peak, DWPF will add less antifoam and has eliminated adding diluted antifoam in SB9 Nitric-Glycolic Acid processing.<sup>59</sup>

Mixing could influence tests investigating foaming. When gas forms in the SRAT and SME, the gas bubbles will coalesce and rise to the top of the vessel. The shear produced by the impellers could cause the gas bubbles to decrease in size, increasing their tendency to foam and making any foam that formed more stable. If investigating foaming at multiple scales, the mixing systems should be designed to provide comparable shear at all scales.

**Table 3-11. SRAT and SME Antifoam Strategy for Nitric-Glycolic Acid and Nitric-Formic Acid Flowsheets, gallons undiluted antifoam**

	Nitric-Formic Acid		Nitric-Glycolic
	SB6#	SB8*	Acid SB9
Prior to presample concentration	1	1	0.25
Presample Concentration each hour	0.5	0.5	0
Prior to ARP Addition	1.2/0.6	0.5	0.25
Prior to nitric acid addition	1.2	0	0
At pH 10 (during nitric)	0	0	0.25
Prior to reducing acid addition	0.6	1.5	NA
Prior to SRAT boiling	3.6	1.5	0.25
Every 12 hours during SRAT	0.6	1	0.25
Prior to Canister Decon Addition	0.6	0.5	0.25
Prior to SME boiling	0.6	0.5	0.25
Prior to frit addition	0.6	1	0.25

# Antifoam was added as a 1 g antifoam in 20 g solution (prepared in large batch in Add Mix Feed Tank)

\* Addition of 100 gallons of water followed each undiluted antifoam addition

Foaming is a liquid surface phenomena so the cross sectional area determines the flux at the surface.<sup>60</sup> If the volume scaled boilup rate is held constant, the larger the scale of the test, the larger the flux at boiling. Therefore, when processing at full-scale, offgas (or boiling) flux is higher than processing in smaller equipment if boilup rate is scaled volumetrically. The boiling flux is summarized in Table 3-12. Although an antifoam addition strategy was developed and demonstrated in 4-L testing with actual and simulated waste, the processing of actual waste in DWPF at the higher flux may require more frequent antifoam additions or larger antifoam additions.

**Table 3-12. Calculated Boiling Flux in SRAT for Scaled Experiments**

	4-L	22-L	220-L	DWPF	
SRAT Diameter	5.9 inches	11.6 inches	23.2 inches	12 ft	
Boilup Rate	2.71 g/min*	15.69 g/min*	102.39 g/min*	2,500 lb/hr	5,000 lb/hr
Boiling Flux, lb/hr/ft <sup>2</sup>	2.90	5.08	7.37	22.1	44.2

\* Boilup rate calculated from design basis boilup of 5,000 lb/hr in DWPF

Testing was completed in a 1/240<sup>th</sup> scale SRAT with oversized steam coils to achieve the design basis boiling flux (5,000 lb/hr DWPF or 90 lb/hr steam in this pilot SRAT). This equipment was used primarily to demonstrate the effectiveness of Antifoam 747<sup>61,62</sup> prior to its implementation in DWPF. It also demonstrated that Antifoam 747 was effective at DWPF design basis steam flow.

Foaming is influenced by the rheological properties and impacted by the size and surface activity of insoluble solids. Where foaming is an essential component, the simulant would have to be adjusted to replicate the key foaming properties versus the chemistry as has been done for flowsheet development. Larger scale testing was also used to replicate the boiling flux during DWPF operation.

### 3.8 Processing Window for the Nitric-Glycolic Acid Flowsheet

For the Nitric-Glycolic Acid flowsheet, nitrite is destroyed, even at low acid stoichiometry, and hydrogen generation is very low. So, neither of these is important in developing the flowsheet. Instead, rheology, mercury stripping, and solids concentration are the parameters that will affect the processing window and targeted acid stoichiometry.

In simulant and actual waste testing, the yield stress and apparent viscosity are acceptable at low and moderate acid stoichiometry for both the SRAT and SME products. The lower end of the acid stoichiometry window is likely below 80% Koopman Minimum Acid stoichiometry<sup>63</sup> (KMA). The upper end of the acid stoichiometry window is the region where both the yield stress and apparent viscosity begin to increase rapidly with a small increase in acid stoichiometry. The upper region can be extended by decreasing the total solids of the SRAT and SME products. This will make them more processable in the CPC but will slow down processing in the melter due to wasting energy to evaporate the excess water. Processing at low acid stoichiometry is preferred, as it will lead to lower offgas generation in the melter. For SB9 simulant testing, the flowsheet window extended from about 80-120% KMA for SRAT product total solids of 20 wt % and SME product total solids of 48 wt %.<sup>38</sup>

In simulant testing, higher acid stoichiometry generally results in higher recovery of elemental mercury in the MWWT. Since mercury recovery in DWPF is the primary purge point for mercury, processing at higher acid stoichiometry might lead to shorter processing time and higher mercury removal.

The Nitric-Glycolic Acid flowsheet processing window, like all previous Nitric-Formic Acid flowsheets, should be developed based on simulant experiments. A radioactive demonstration is recommended to ensure there is no minor component in sludge, ARP product or strip effluent that was not present in simulant experiments that impacts processing. No pilot or semiworks testing are needed in developing the Nitric-Glycolic Acid flowsheet. Development of the optimum flowsheet will become more challenging as higher volumes of strip effluent and ARP are processed once the Salt Waste Processing Facility begins operation.

This report summarized the previous work completed in developing the flowsheet for SB6 and SB8 and compared the processing in 4-L experiments with simulants, in 1-L experiments with actual waste, and in batch processing in DWPF.



- Flowsheet development for the Nitric-Glycolic Acid flowsheet should use the same testing philosophy, although the operating window will be determined by rheology since nitrite destruction is no longer necessary and hydrogen generation is very low.

#### Recommendations for future testing to develop DWPF flowsheets:

The best test conditions for the development of future Nitric-Glycolic Acid flowsheets are:

- Develop the processing window using nonradioactive Tank 40, PRFT, and SEFT chemical simulant experiments followed by one experiment with actual sludge, actual PRFT, and simulated SEFT. Since rheology is key to defining the operating window, complete simulant testing to determine the acid stoichiometry processing window where simulant rheology is acceptable and use actual waste experiment to verify rheology is acceptable at processing target. Determine anion destruction factors for prediction of REDOX. Measure glass REDOX and characterize liquid and offgas concentrations throughout processing.
- Use prototypic operating conditions (air purge, acid addition rate, scaled volumetric boilup rate that DWPF plans to use). Testing at plant operating conditions, not design basis, should not be the condition for most testing, as design basis does not simulate the time at temperature or mercury stripping in DWPF processing.
- Use typical volumes of PRFT and SEFT. Use best PRFT and SEFT simulants (without simulated organic entrainment). No sludge-only testing is warranted unless sludge-only processing is planned in DWPF
- Use expected mercury concentration and mercury speciation to demonstrate elemental mercury stripping efficiency and expected mercury speciation in SRAT and SME products and condensate.

## 4.0 Conclusions

The DWPF is planning to modify the chemical processing flowsheet by replacing formic acid with glycolic acid<sup>37</sup> in the CPC SRAT and SME. The replacement of formic acid with glycolic acid virtually eliminates the CPC's largest flammability hazards: catalytic hydrogen and ammonia.

Prior to DWPF startup, full, semiworks, pilot and laboratory scale testing were completed to understand the chemistry and engineering of radioactive waste processing. Actual waste experiments up to 25-L were performed. Since the DWPF radioactive startup in March 1996, a Nitric-Formic Acid operating window has been developed for each of the eleven sludge batches based on 4-L simulant experiments and a single ~1-L radioactive demonstration. Although pilot-testing was instrumental in the initial design and flowsheet development for the DWPF, pilot-scale testing has not been used to develop the CPC operating window during radioactive processing. This is true even for the incorporation of new salt processing effluents into the DWPF process (i.e., Actinide Removal Process in 2007 and the Modular Caustic-Side Solvent Extraction Unit in 2008).

This report concludes that the process chemistry from laboratory to full-scale is essentially the same in simulant testing, in an actual waste demonstration, and during the DWPF processing of each sludge batch. In both laboratory experiments and the DWPF, mixing and heat transfer are adequate to mix immiscible liquids, organics and insoluble solids.

Extensive testing has been completed to develop the Nitric-Glycolic Acid CPC flowsheet. Over 100 simulations have been completed to understand the keys to chemical processing. Testing has been completed at three different scales including laboratory testing in 4-L and 22-L processing equipment along with testing in a geometrically scaled 220-L (~1/216<sup>th</sup>) pilot-scale equipment. The testing utilized non-radioactive simulants of various sludge batches as well as a matrix of simulants designed to bound the compositional range of sludge solids. In addition, a small number of 1-L tests have been performed with samples of radioactive tank waste.

A SB9 simulant was used to develop the first sludge batch specific Nitric-Glycolic Acid CPC operating window. CPC simulations were completed using sludge simulant, Strip Effluent Feed Tank simulant and Precipitate Reactor Feed Tank simulant. Ten sludge-only SRAT cycles and four SRAT/SME cycles were completed. In addition, one actual SB9 sludge-only SRAT and SME cycle was completed as part of the SB9 flowsheet process development. The actual SB9 test validated the equivalency of the simulant testing protocol.

The same testing philosophy that is used for the Nitric-Formic Acid flowsheet is also recommended for development of an operating window for the Nitric-Glycolic Acid flowsheet, namely that development be based on a series of simulant experiments and a radioactive demonstration. A larger volume radioactive experiment would allow more analyses (particularly rheology) to be completed in better understanding the extended processing that will be needed after the SWPF startup. The recommended processing target for the actual waste experiment and for the DWPF processing is based on maximizing solids concentration (to maximize melter efficiency) and mercury removal.

## **5.0 Recommendations**

The following recommendations cover both the testing needed to develop future Nitric-Glycolic Acid flowsheets and the processing conditions for optimum processing in DWPF.

Detailed testing conditions for Nitric-Glycolic Acid flowsheet are discussed in Section 3.8. This includes developing the flowsheet using chemical simulants, testing at prototypic conditions, characterizing the liquid and offgas concentrations throughout processing, and adding various forms of mercury to duplicate that present in the actual waste. Measurement of slurry rheology, anion destruction factors for prediction of REDOX, and glass REDOX are recommended for all experiments used to determine the processing window. The processing window will be defined to span the area where rheology is acceptable within the REDOX bounds of 0.09-0.33.

The recommended processing target for the actual waste experiment and DWPF will be selected to maximize solids concentration (to maximize melter efficiency) and mercury removal. A single demonstration with actual waste (sludge, PRFT and SEFT) will verify that processing proceeds as predicted by simulant testing.

## 6.0 References

1. Barnes, M. J.; Peterson, R. A. *Excess Sodium Tetraphenylborate and Intermediates Decomposition Studies*; WSRC-TR-98-00099, Revision 1; Savannah River Technology Center, Aiken, SC, 1998.
2. Smith, M. E.; Hutson, N. D.; Miller, D. H.; Morrison, J.; Shah, H. B.; Shuford, J. A.; Glascock, J.; Wurzinger, F. H.; Zamecnik, J. R. *Checkout and Start-up of the Integrated DWPF Melter System*; WSRC-RP-89-321; Savannah River Technology Center, Aiken, SC, 1989.
3. Ritter, J. A.; Hutson, N. D.; Smith, M. E.; Andrews, M. K.; Miller, D. H.; Zamecnik, J. R. *Integrated DWPF Melter System Campaign Report Coupled Feed Operation*; WSRC-TR-90-131, Revision 0; Savannah River Technology Center, Aiken, SC, 1990.
4. Hutson, N. D.; Zamecnik, J. R.; Smith, M. E.; Miller, D. H.; Ritter, J. A. *Integrated DWPF Melter System (IDMS) Campaign Report: Mercury Operation*; WSRC-TR-91-0363; Savannah River Technology Center, Aiken, SC, 1991.
5. Hutson, N. D.; Zamecnik, J. R.; Smith, M. E.; Miller, D. H.; Ritter, J. A. *Integrated DWPF Melter System Campaign Report: The First Two Noble Metals Operations*; WSRC-TR-91-0400; Savannah River Technology Center, Aiken, SC, 1991.
6. Zamecnik, J. R.; Hutson, N. D.; Smith, M. E.; Miller, D. H.; Ritter, J. A. *Integrated DWPF Melter System (IDMS) Campaign Report - DWPF Cold Run Demonstrations*; WSRC-RP-93-593, Revision 0; Savannah River Technology Center, Aiken, SC, 1993.
7. Hutson, N. D. *An Evaluation of Mercury Removal in the IDMS Using the Nitric Acid Flowsheet*; WSRC-TR-92-492; Savannah River Technology Center, Aiken, SC, 1992.
8. Hutson, N. D.; Zamecnik, J. R. *Integrated DWPF Melter System (IDMS) Campaign Report: IDMS PUREX-6 (PX6) Operation*; WSRC-TR-94-0556, Revision 0; Savannah River Technology Center, Aiken, SC, 1994.
9. Lambert, D. P. *Ammonia Scrubber Testing During IDMS SRAT and SME processing*; WSRC-TR-94-8000, Revision 1; Savannah River Technology Center, Aiken, SC, 1995.
10. Randall, C. T.; Papouchado, L. M.; Marra, S. L. *The Defense Waste Processing Facility, from Vision to Reality*; WSRC-MS-2000-00111; Savannah River Technology Center, Aiken, SC, 2000.
11. Carter, J. T.; Edwards, R. E.; Occhipinti, J. E.; Beck, R. S.; Iverson, D. C. *Defense Waste Processing Facility Radioactive Operations Year Two*; Waste Management 1998/14-03/; Westinghouse Savannah River Company, Aiken, SC, 1998.
12. Fellingner, T. L.; Marshall, K. M.; Bibler, N. E.; Crawford, C. L. *Confirmation Run of the DWPF SRAT Cycle Using the Sludge-Only Flowsheet with Tank 42 Radioactive Sludge and Frit 200 in the Shielded Cells Facility*; WSRC-RP-98-00329, Revision 0; Savannah River Technology Center, Aiken, SC, 1998.
13. Koopman, D. C. *Sludge Batch 2 (Macrobatches 3) Flowsheet Studies with Simulants*; WSRC-TR-2000-00398, Revision 0; Savannah River Technology Center, Aiken, SC, 2000.
14. Fellingner, T.; Pareizs, J. M.; Bibler, N. E.; Cozzi, A. D.; Crawford, C. L. *Confirmation Run of the DWPF SRAT Cycle Using the Sludge-Only Flowsheet with Tank 40 Radioactive Sludge and Frit 200*

*in the Shielded Cells Facility*; WSRC-TR-2002-00076; Savannah River Technology Center, Aiken, SC, 2002.

15. Herman, C. C.; Koopman, D. C.; Best, D. R.; Snyder, T. K.; Williams, M. F. *Sludge Batch 3 Simulant Flowsheet Studies: Final Phase SRAT/SME Result*; WSRC-TR-2003-00422, Revision 0; Savannah River Technology Center, Aiken, SC, 2003.
16. Pareizs, J. M.; Koopman, D. C.; Click, D. R.; Cozzi, A. D.; Bibler, N. E. *Sludge Batch 3 Qualification in the SRTC Shielded Cells*; WSRC-TR-2004-00050, Revision 0; Savannah River Technology Center, Aiken, SC, 2004.
17. Herman, C. C.; Best, D. R.; Lambert, D. P.; Stone, M. E.; Williams, M. F. *Sludge Batch 4 Without Tank 4 Simulant Flowsheet Studies: Phase I SRAT Results*; WSRC-TR-2005-00493, Revision 0; Savannah River Technology Center, Aiken, SC, 2005.
18. Pareizs, J. M.; Bannochie, C. J.; Barnes, M. J.; Bibler, N. E.; Click, D. R.; Hansen, E. K.; Lambert, D. P.; Stone, M. E. *Demonstration of the DWPF Flowsheet in the SRNL Shielded Cells in Support of Sludge Batch 4 Qualification*; WSRC-STI-2007-00053, Revision 0; Savannah River National Laboratory, Aiken, SC, 2007.
19. Lambert, D. P.; Stone, M. E.; Pickenheim, B. R.; Best, D. R.; Koopman, D. C. *Sludge Batch 5 Simulant Flowsheet Studies*; SRNS-STI-2008-00024, Revision 0; Savannah River National Laboratory, Aiken, SC, 2008.
20. Pareizs, J. M.; Bannochie, C. J.; Click, D. R.; Lambert, D. P.; Stone, M. E.; Pickenheim, B. R.; Billings, A. L.; Bibler, N. E. *Sludge Washing and Demonstration of the DWPF Flowsheet in the SRNL Shielded Cells for Sludge Batch 5 Qualification*; SRNS-STI-2008-00111, Revision 0; Savannah River National Laboratory, Aiken, SC, 2008.
21. Koopman, D. C.; Best, D. R. *Sludge Batch 6/Tank 5I Simulant Chemical Process Cell Simulations*; SRNL-STI-2010-00173, Revision 0; Savannah River National Laboratory, Aiken, SC, 2010.
22. Pareizs, J. M.; Pickenheim, B. R.; Bannochie, C. J.; Billings, A. L.; Bibler, N. E.; Click, D. R. *Sludge Washing and Demonstration of the DWPF Flowsheet in the SRNL Shielded Cells for Sludge Batch Qualification*; SRNL-STI-2010-00353, Revision 0; Savannah River National Laboratory, Aiken, SC, 2010.
23. Pareizs, J. M.; Billings, A. L.; Click, D. R. *Sludge Washing and Demonstration of the DWPF Flowsheet in the SRNL Shielded Cells for Sludge Batch 7a Qualification*; SRNL-STI-2011-00226, Revision 0; Savannah River National Laboratory, Aiken, SC, 2011.
24. Koopman, D. C. *DWPF Simulant CPC Studies for SB7b*; SRNL-STI-2011-00547, Revision 0; Savannah River National Laboratory, Aiken, SC, 2011.
25. Pareizs, J. M.; Billings, A. L.; Reboul, S. H.; Lambert, D. P.; Click, D. R. *Sludge Batch 7b Qualification Activities with SRS Tank Farm Sludge*; SRNL-STI-2011-00548 Revision 0; Savannah River National Laboratory, Aiken, SC, 2011.
26. Koopman, D. C.; Zamecnik, J. R. *DWPF Simulant CPC Studies for SB8*; SRNL-STI-2013-00106, Revision 0; Savannah River National Laboratory, Aiken, SC, 2013.

27. Pareizs, J. M.; Crawford, C. L. *Sludge Washing and Demonstration of the DWPF Flowsheet in the SRNL Shielded Cells for Sludge Batch 8 Qualification*; SRNL-STI-2013-00116, Revision 0; Savannah River National Laboratory, Aiken, SC, 2013.
28. Smith, T. E.; Newell, J. D.; Woodham, W. H. *Defense Waste Processing Facility Simulant Chemical Processing Cell Studies for Sludge Batch 9*; SRNL-STI-2016-00281, Revision 0; Savannah River National Laboratory, Aiken, SC, 2016.
29. Newell, J. D.; Pareizs, J.; Martino, C. J.; Reboul, S. H.; Coleman, C. J.; Edwards, T. B.; Johnson, F. C. *Actual Waste Demonstration of the Nitric-Glycolic Flowsheet for Sludge Batch 9 Qualification*; SRNL-STI-2016-00327, Revision 1; Savannah River National Laboratory, Aiken, SC, 2017.
30. Ferrara, D. M.; Ha, B. C.; Lambert, D. P.; Bibler, N. E. *Technical Assessment of a Sludge-Only Frit 200 Flowsheet with Copper*; WSRC-TR-96-0142; Savannah River Technology Center, Aiken, SC, 1996.
31. Baich, M. A.; Herman, C. C.; Eibling, R. E.; Williams, M. F.; Smith, F. G. *Sludge Batch 4 Simulant Flowsheet Studies with ARP and MCU: Impact of MCU Organics*; WSRC-TR-2005-00230, Revision 0; Savannah River National Laboratory, Aiken, SC, 2005.
32. Pickenheim, B. R.; Stone, M. E.; Newell, J. D. *Glycolic - Formic Acid Flowsheet Development*; SRNL-STI-2010-00523, Revision 0; Savannah River National Laboratory, Aiken, SC, 2010.
33. Lambert, D. P.; Koopman, D. C. *Glycolic-Formic Acid Flowsheet Sludge Matrix Study*; SRNL-STI-2011-00275, Revision 0; Savannah River National Laboratory, Aiken, SC, 2011.
34. Lambert, D. P.; Zamecnik, J. R.; Best, D. R. *FY13 Glycolic-Nitric Acid Flowsheet Demonstrations of the DWPF Chemical Process Cell with Simulants*; SRNL-STI-2013-00343, Revision 0; Savannah River National Laboratory, Aiken, SC, 2014.
35. Lambert, D. P.; Zamecnik, J. R.; Newell, J. D.; Martino, C. J. *Impact of Scaling on the Glycolic-Nitric Acid Flowsheet*; SRNL-STI-2014-00306; Savannah River National Laboratory, Aiken, SC, 2016.
36. Martino, C. J.; Newell, J. D.; Williams, M. *Nitric-Glycolic Flowsheet Testing for Maximum Hydrogen Generation Rate*; SRNL-STI-2015-00130, Revision 0; Savannah River National Laboratory, Aiken, SC, 2016.
37. Lambert, D. P. *SB9 Nitric-Glycolic Acid Flowsheet Development*, eNotebook Experiment ID o7787-00055-19, Savannah River National Laboratory, Aiken, SC, 2016.
38. Lambert, D. P.; Williams, M. S.; Brandenburg, C. H.; Luther, M. C.; Newell, J. D.; Woodham, W. H. *Sludge Batch 9 Simulant Runs Using the Nitric-Glycolic Acid Flowsheet*; SRNL-STI-2016-00319, Revision 0; Savannah River National Laboratory, Aiken, SC, 2016.
39. Martino, C. J.; Newell, J. D.; Crawford, C.; Pareizs, J.; Williams, M. S. *Sludge Batch 9 Follow-on Actual-Waste Testing for the Nitric-Glycolic Flowsheet*; SRNL-STI-2016-00726, Revision 0; Savannah River National Laboratory, Aiken, SC, 2017.
40. Lambert, D. P.; Pareizs, J.; Click, D. R. *Demonstration of the Glycolic-Formic Flowsheet in the SRNL Shielded Cells Using Actual Waste*; SRNL-STI-2011-00622, Revision 0; Savannah River National Laboratory, Aiken, SC, 2011.

41. Holtzscheiter, E. W. *Response to the Independent Technology Review (ITR) Report - Nitric-Glycolic Acid Flowsheet for the DWPF At the Savannah River Site*; SRR-WSE-2017-00038, Revision 0; 2017.
42. Holtzscheiter, E. W., Clarification of Task 2.f per the email option specified in HLW-DWPF-TTR-2013-0003, Rev 0. Savannah River Remediation LLC: Aiken, SC, 2017.
43. *Conduct of Engineering Technical Reviews, Manual E7, Procedure 2.60, Revision 17*; Savannah River Site: Aiken, SC, 2016.
44. *Savannah River National Laboratory Technical Report Design Check Guidelines*; WSRC-IM-2002-00011, Revision 2; Savannah River National Laboratory, Aiken, SC, 2004.
45. Knipe, A. C.; Watts, W. E., *Organic Reaction Mechanisms*. 1988, 176-226.
46. Zabetakis, M. G. *Flammability Characteristics of Combustible Gases and Vapors*; Bulletin 627; US Department of Interior, Bureau of Mines, Washington DC, 1965.
47. Koopman, D. C. *DWPF Hydrogen Generation Study-Form of Noble Metal SRAT Testing*; WSRC-TR-2005-00286; Savannah River National Laboratory, Aiken, SC, 2005.
48. Jamison, L. C. *DWPF-SRNL Catalytic Hydrogen Information*; X-ESR-S-00373, Revision 0; Savannah River Remediation, LLC, Aiken, SC, 2018.
49. Koopman, D. C.; Best, D. R.; Pickenheim, B. R. *SRAT Chemistry and Acid Consumption during Simulated DWPF Melter Feed Preparation*; WSRC-STI-2008-00131, Revision 0; Savannah River National Laboratory, Aiken, SC, 2008.
50. Jantzen, C. M.; Williams, M. S.; Edwards, T. B.; Trivelpiece, C. L.; Ramsey, W. G. *Nitric-glycolic Flowsheet Reduction/Oxidation (REDOX) Model for the Defense Waste Processing Facility (DWPF)*; SRNL-STI-2017-00005, Revision 0; Savannah River National Laboratory, Aiken, SC, 2017.
51. Jantzen, C. M. *Heat Treatment of Waste Slurries for REDOX and Corrosion Analyses*; Manual L29, Procedure ITS-0052, Rev. 5; Savannah River National Laboratory, Aiken, SC, 2016.
52. Wingard, B. R. *Path Forward to Address the Mercury Balance at the DWPF and Determine How to Recover, Transfer, and Purify Mercury in the CPC*; SRR-WSE-2010-00077; Savannah River Remediation LLC, Aiken, SC, 2010.
53. Bricker, J. M. *Path Forward to Address Reduction of SRAT Cycle Time Via Increasing the Current Mercury Processing Limit*; SRR-WSE-2010-00001; Savannah River Remediation, LLC, Aiken, SC, 2010.
54. Lambert, D. P.; Zamecnik, J. R.; Pareizs, J. M.; Coleman, C. J. *Analysis of DWPF CPC Mercury Samples*; SRNL-STI-2014-00583; Savannah River National Laboratory, Aiken, SC, 2014.
55. Fellingner, T.; Bannochie, C. J. *Phase 2 Report-Mercury Behavior in the Defense Waste Processing Facility*; X-ESR-S-00279, Revision 1; Savannah River Remediation, LLC, Aiken, SC, 2016.
56. Marinik, A. R.; Stone, M. E. *Evaluation of Mixing in the Slurry Mix Evaporator and Melter Feed Tank*; WSRC-TR-2004-00436, Revision 0; Savannah River National Laboratory, Aiken, SC, 2004.

57. Kreith, F.; Black, W. Z., *Basic Heat Transfer*. Harper & Row: 1980.
58. Lambert, D. P.; Koopman, D. C.; Newell, J. D.; Wasan, D. T.; Nikolov, A. P.; Weinheimer, E. K. *Improved Antifoam Agent Study End of Year Report, EM Project 3.2.3*; SRNL-STI-2011-00515, Revision 0; Savannah River National Laboratory, Aiken, SC, 2011.
59. Clark, M. C. *Alternate Defoamer Development for CPC Processing*; X-TTR-S-00046, Revision 1; Savannah River Remediation, LLC, Aiken, SC, 2017.
60. Wasan, D. T.; Lambert, D. P. *Foaming and Antifoaming in Radioactive Waste Pretreatment and Immobilization*; Project Number: 60143; Illinois Institute of Technology, Chicago, IL, 2001.
61. Koopman, D. C. *Comparison of Dow Corning 544 Antifoam to IIT747 Antifoam in the 1/240 SRAT*; WSRC-TR-99-00377; Savannah River Technology Center, Aiken, SC, 2000.
62. Koopman, D. C. *Hydrogen Generation and Foaming during Tests in the GFPS Simulating DWPF Operations with Tank 42 Sludge and CST*; WSRC-TR-99-00302, Rev. 1; Savannah River Technology Center, Aiken, SC, 2001.
63. Koopman, D. C.; Pickenheim, B. R.; Lambert, D. P.; Newell, J. D.; Stone, M. E. *Characterization of Individual Chemical Reactions Consuming Acid during Nuclear Waste Processing at the Savannah River Site - 136B*; SRNL-L3100-2009-00219; Savannah River National Laboratory, Aiken, SC, 2009.
64. Elson, T. P.; Cheesman, D. J.; Nienow, A., X-Ray Studies of Cavern Sizes and Mixing Performance with Fluids Possessing a Yield Stress. *Chem. Eng. Sci.* 1986, *41* (10), 2555-2562.
65. Elson, T. P., The Growth of Caverns Formed Around Rotating Impellers During the Mixing of A Yield Stress Fluid. *Chem. Eng. Comm.* 1990, *96* (1), 303-319.
66. Etchells, A. W.; Ford, W. N.; Short, D. G. R., Mixing of Bingham Plastics on an Industrial Scale. *Fluid Mixing III: The Institution of Chemical Engineers Symposium Series No. 108* 1987, 271-285.
67. Amerine, D. B. *Basic Data Report Defense Waste Processing Facility Sludge Plant Savannah River Site 200-S Area*; WSRC-RP-92-1186, Revision 139; Westinghouse Savannah River Company, Aiken, SC, 1992.
68. Garrison, C. M., How to Design and Scale Mixing Pilot-Plants. *Chem. Eng.* February 7, 1983, 63-70.
69. Poirier, M.; Herman, D.; Fondeur, F. F.; Hansen, E. K.; Fink, S. D. *MST/Sludge Agitation Studies for Actinide Removal Process and DWPF*; WSRC-TR-2003-00471, Revision 0; Savannah River Technology Center, Aiken, SC, 2003.





## Appendix A -- Email Requesting This Task

### Clarification of Task 2.f. per the email option specified in HLW-DWPF-TTR-2013-0003, Rev. 0

**Bill Holtzscheiter** to: Frank Pennebaker, Chris Martino, Dan Lambert  
Cc: Eric Freed, Victoria Kmiec, Terri Fellingner, Thomas Colleran

02/08/2017 07:12 AM

History: This message has been replied to.

		Bill Holtzscheiter	Clarification of Task 2.f. per the email option specified in HLW-DWPF-TTR-2
		Dan Lambert	<i>Bill Thanks.</i>

Clarification of Task 2.f. per the email option specified in HLW-DWPF-TTR-2013-0003, Rev. 0

As discussed in the "Background" section of HLW-DWPF-TTR-2013-0003 Rev. 0. historical performance of small scale testing has been the basis for scaling from 1 liter, 4 liter and 22 liter testing to full DWPF scale. To address a comment from the recent Independent Technology Review (ITR) of the Nitric-Glycolic Acid flowsheet, please document the scaling performance of historical testing for the Nitric-Formic Acid flowsheet utilizing laboratory scale, Integrated DWPF Melter System (IDMS), scale melter, and DWPF cold and radioactive runs.. As part of this documentation, this scaling rationale should be applied to the Nitric-Glycolic Acid flowsheet. This does not require a revision of the Task Technical and Quality Assurance Plan since it is within the scope as defined in SRNL-RP-2012-00762, Rev. 0. This email scope clarification shall be documented in the appropriate SRNL laboratory notebook and included as an attachment to the technical report.

Deliverable: A stand-alone technical report documenting the historical performance of scaling from laboratory to bench to large pilot to full scale for the DWPF process. Performance is based on the Nitric-Formic Acid flowsheet with the technical basis for extending the scaling process to the Nitric-Glycolic Acid flowsheet.

Victoria Kmiec will work with SRNL to determine funding allocation and priority.

Bill Holtzscheiter  
Flowsheet Engineering  
Office: 803-725-6722  
Cell: 803-645-4107



## Appendix B – Offgas Hydrogen Data

Detailed Offgas charts for each run for hydrogen are included in this appendix.

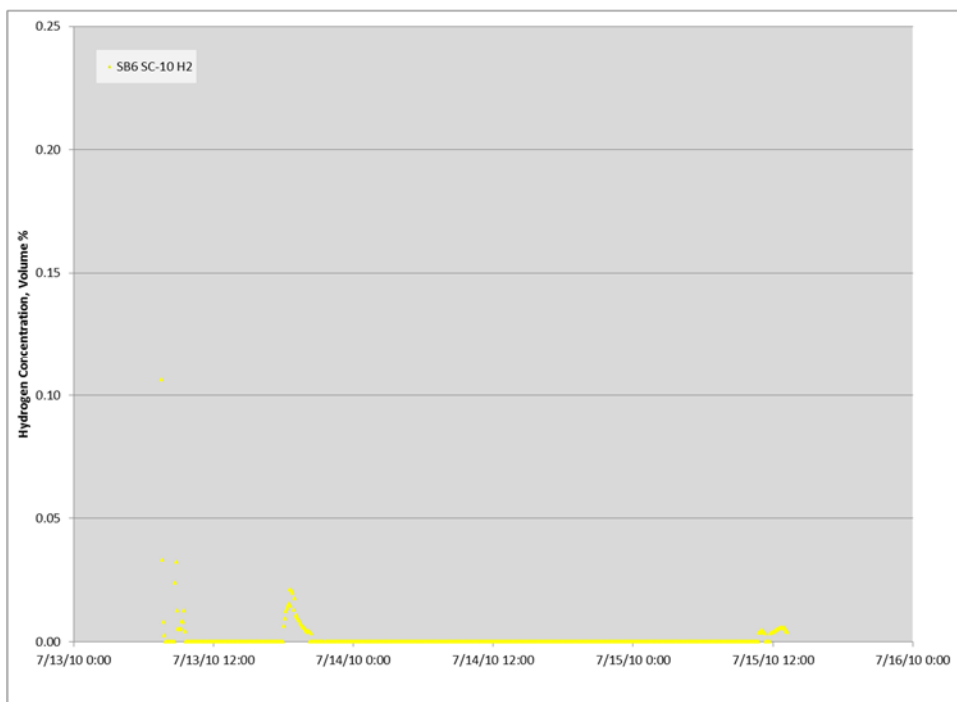


Figure B-1. SC-10 SRAT Hydrogen

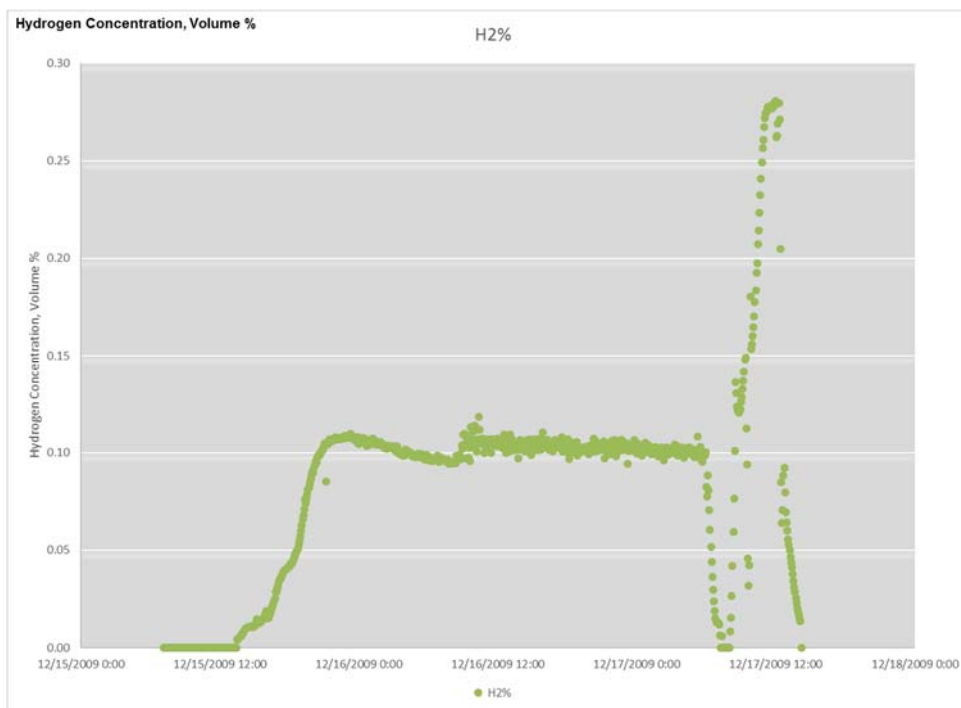
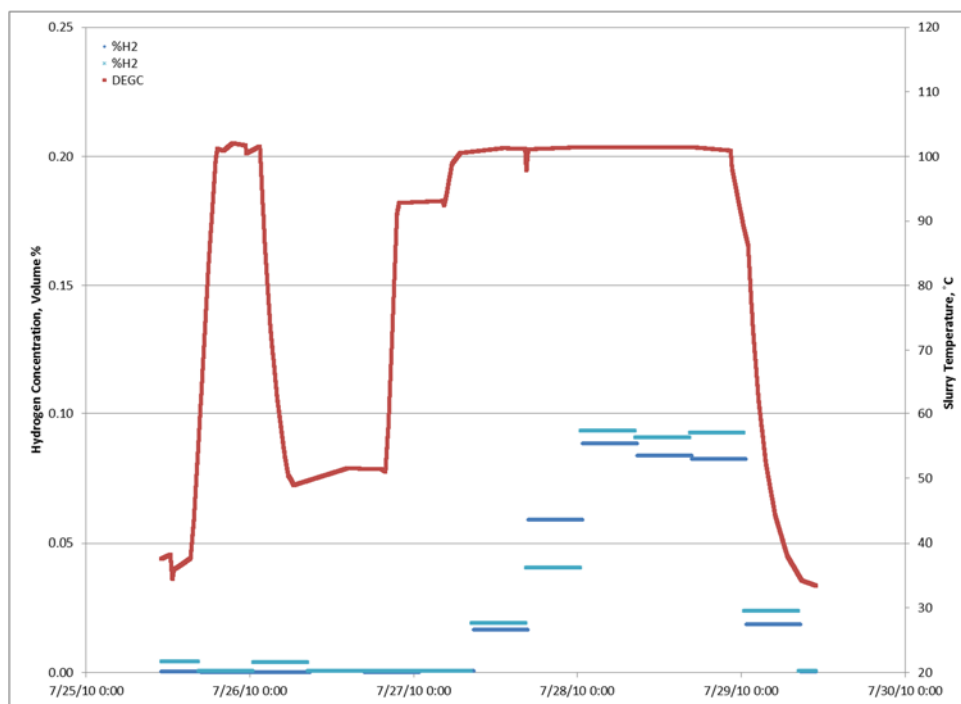
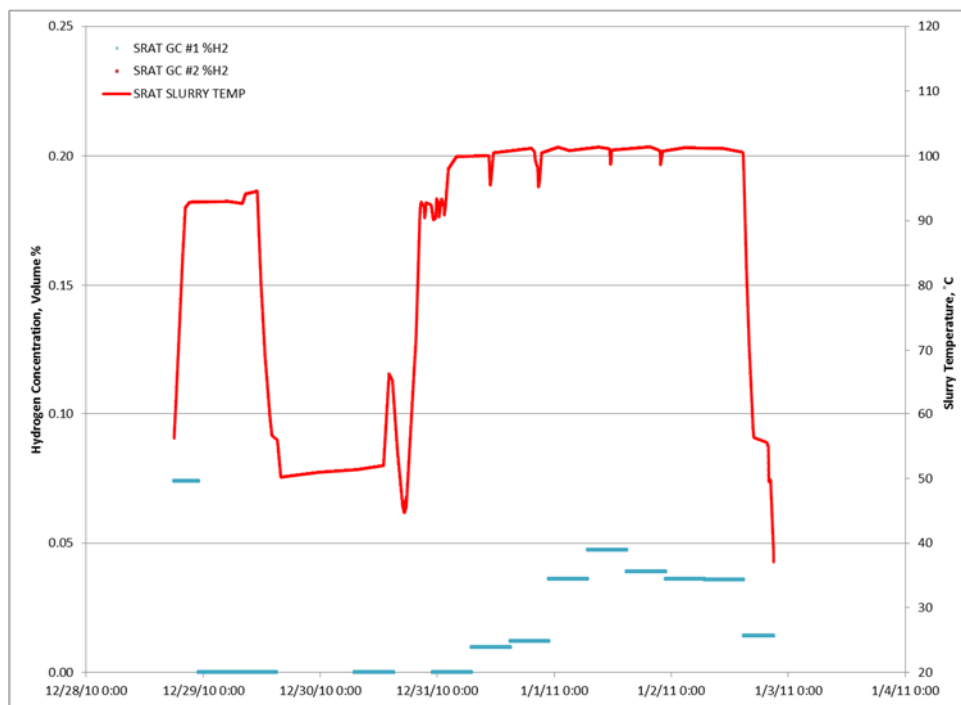


Figure B-2. SB6-14 SRAT Hydrogen

**Figure B-3. DWPF Batch 535 SRAT Hydrogen****Figure B-4. DWPF Batch 555 SRAT Hydrogen**

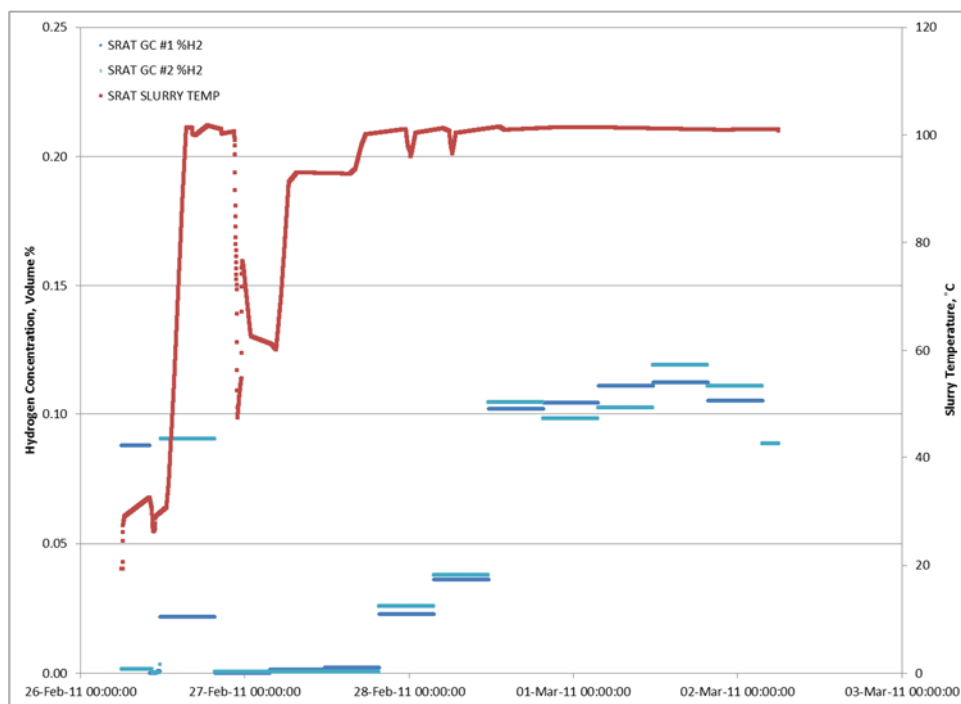


Figure B-5. DWPF Batch 565 SRAT Hydrogen

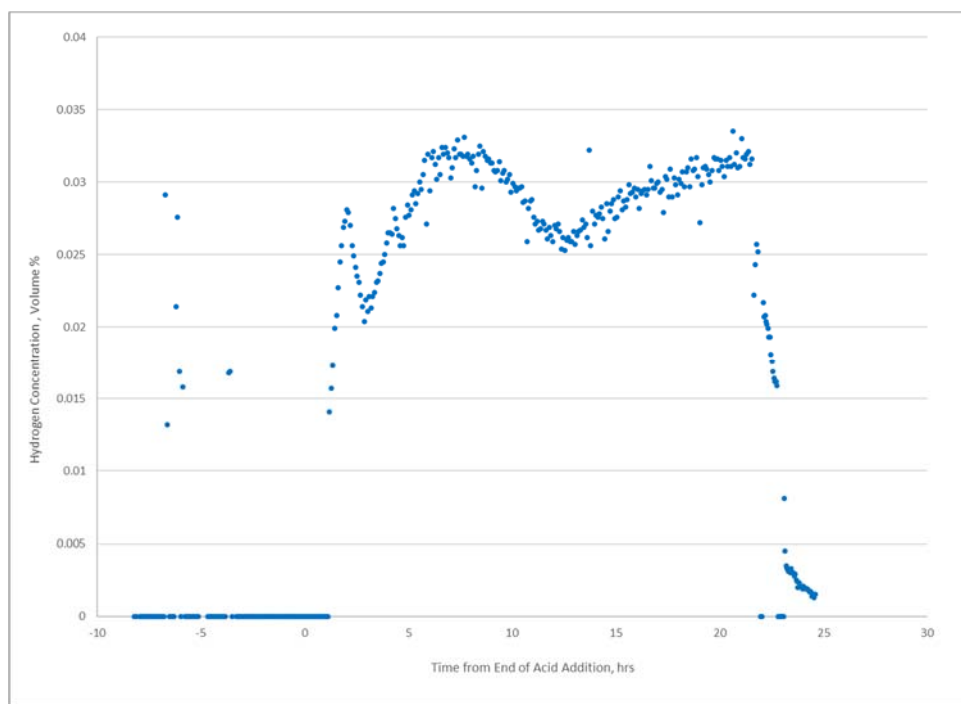


Figure B-6. SC-14 SRAT Hydrogen

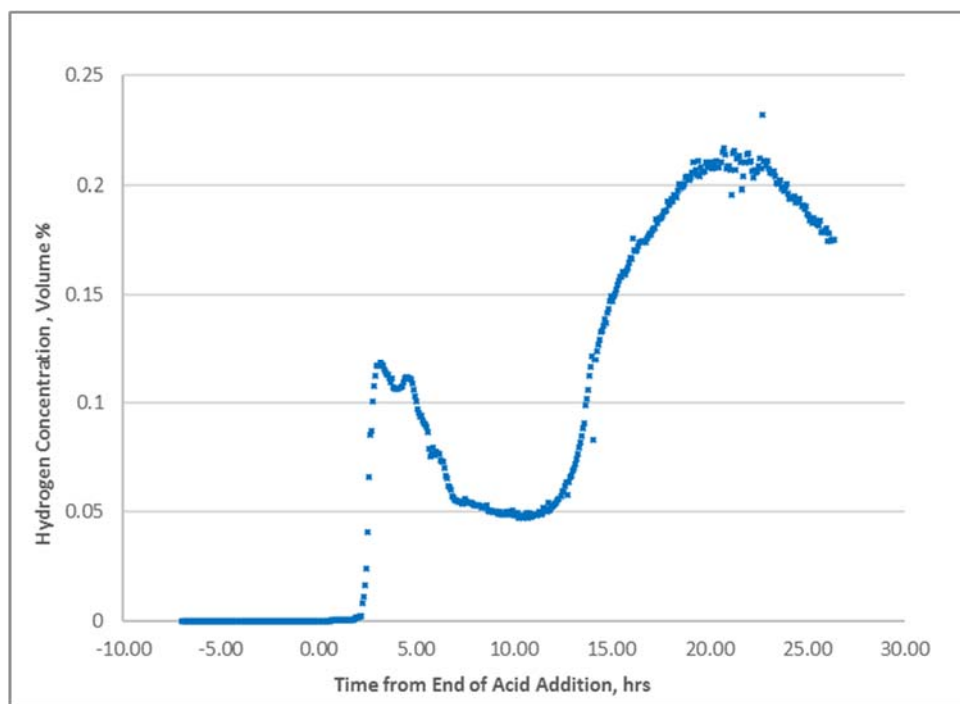


Figure B-7. SB8-A2 SRAT Hydrogen

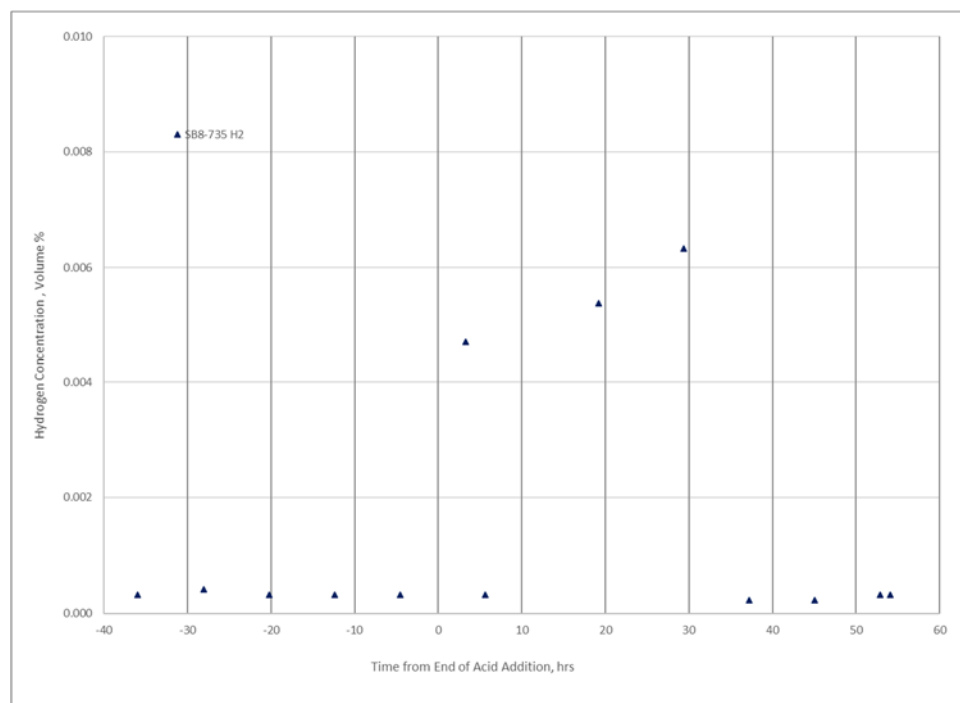
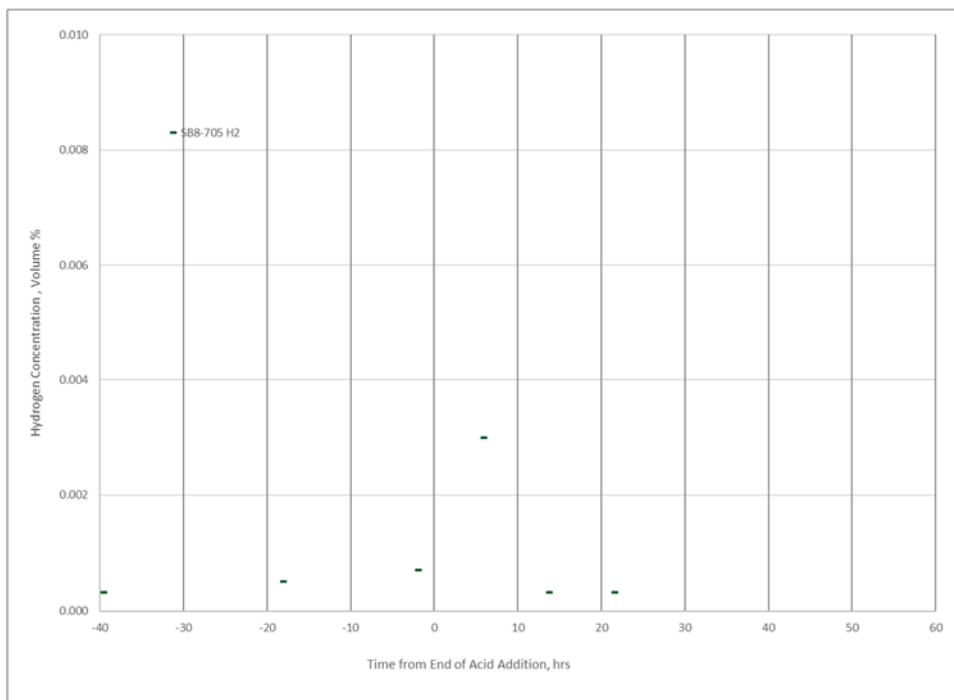
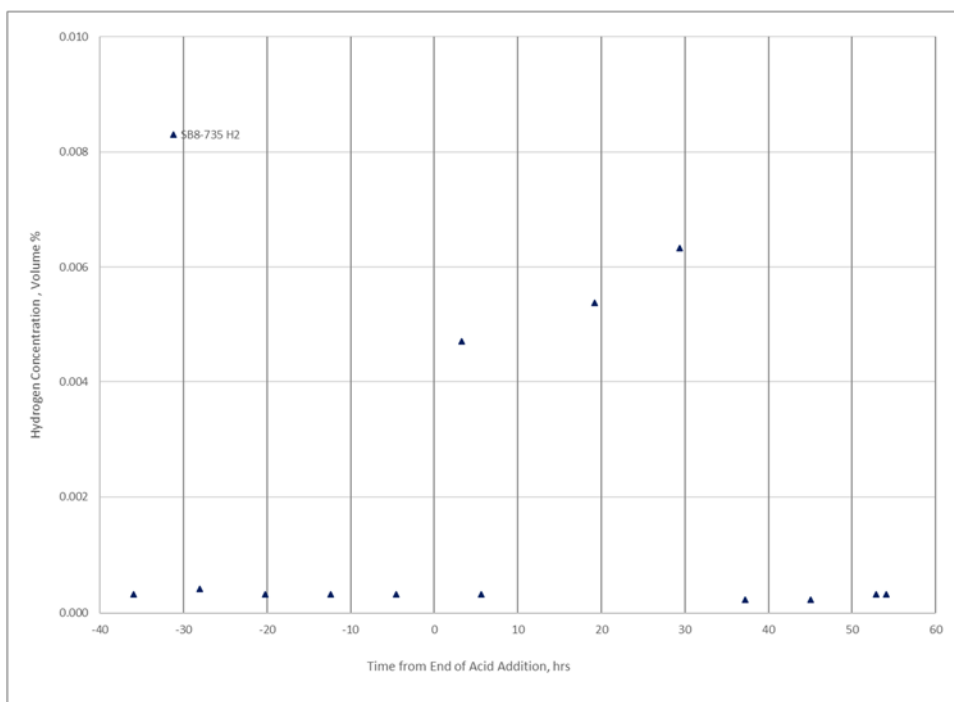


Figure B-8. DWPF Batch 680 SRAT Hydrogen



**Figure B-9. DWPF Batch 705 SRAT Hydrogen**



**Figure B-10. DWPF Batch 735 SRAT Hydrogen**

### Appendix C—Physical Parameters of Interest

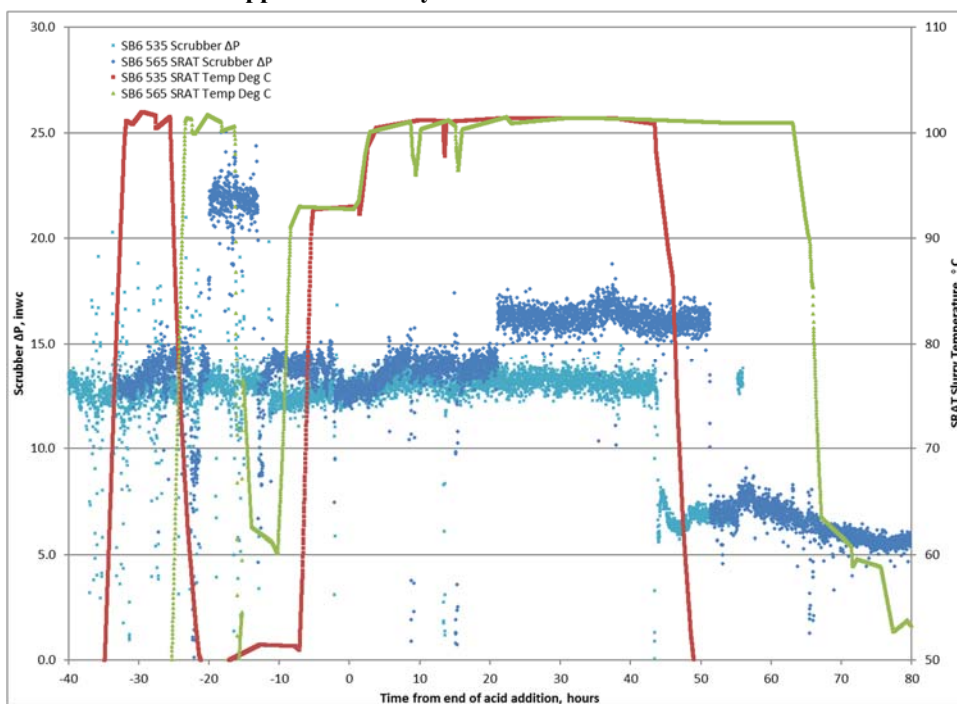


Figure C-1. DWPF SB6 SRAT Scrubber ΔP, inwc

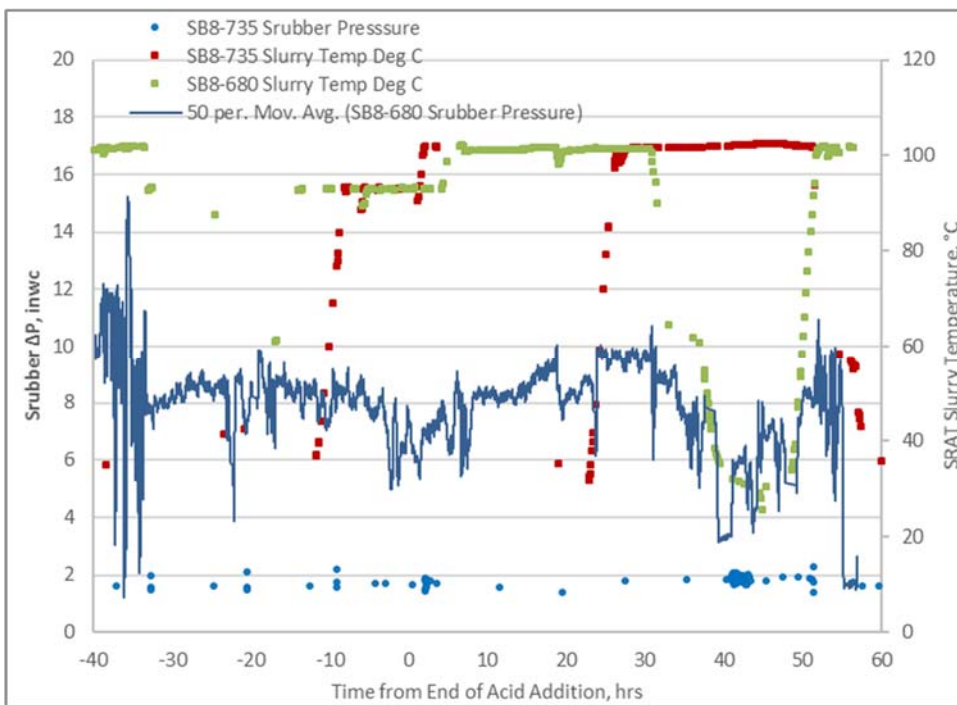


Figure C-2 DWPF SB8 SRAT Scrubber ΔP, inwc

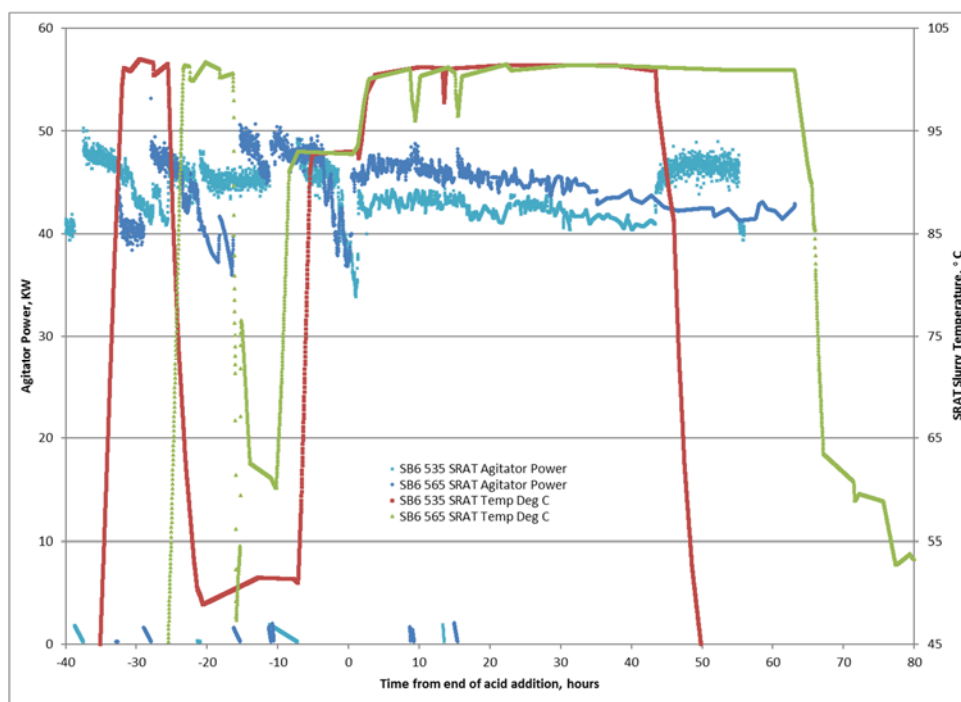


Figure C-3 DWPF SB6 SRAT Agitator Power, KW

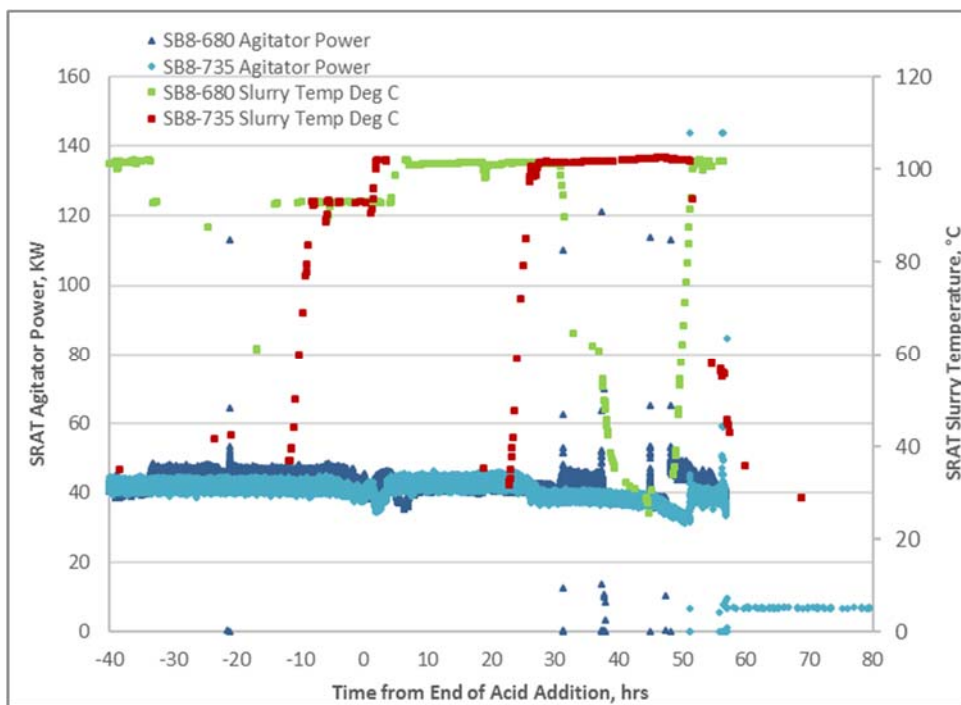


Figure C-4 DWPF SB8 SRAT Agitator Power, KW

## Appendix D—Cavern Mixing Analysis

The objective of mixing is to homogenize the tank and to prevent poorly mixed areas in the SRAT or SME. This prevents the accumulation of added acids, strip effluent, PRFT concentrate, or frit that frequently leads to poor reaction kinetics and inhomogeneous slurries. It also allows representative sampling, which is needed to demonstrate that batch goals are met and to predict that glass quality will be acceptable.

Mixing objectives for the DWPF include the following.

- Miscible liquid blending. Examples of miscible liquid blending include acid addition for anion destruction and hydrogen generation. While hydrogen generation is not caused by mixing, insufficient mixing in DWPF vessel will lower the kinetics of the chemical reactions that lead to hydrogen generation.
- Solid suspension. Since the feed to the SRAT and SME contains insoluble solids, the solids must be adequately suspended to participate in chemical reactions (e.g., mercury reduction to elemental mercury or catalytic reactions). In addition, the immiscible liquids such as elemental mercury must be suspended so that it can participate in the steam stripping.
- Mixing of Bingham plastic fluids. Because of its high insoluble solids concentration, the feed to the SRAT and SME behaves as a Bingham plastic fluid. When mixing a Bingham plastic fluid, it can form a cavern around the impeller, in which the material within the cavern is moving vigorously and is well mixed, and the material outside the cavern is stagnant<sup>64,65,66</sup>. The mixing system should be designed so that the cavern covers the entire working volume of the vessel. The SRAT rheology design basis is 1.5-5 Pa and 5 to 12 cp. The SME rheology design basis is 2.5-15 Pa and 10 to 40 cp.<sup>67</sup>

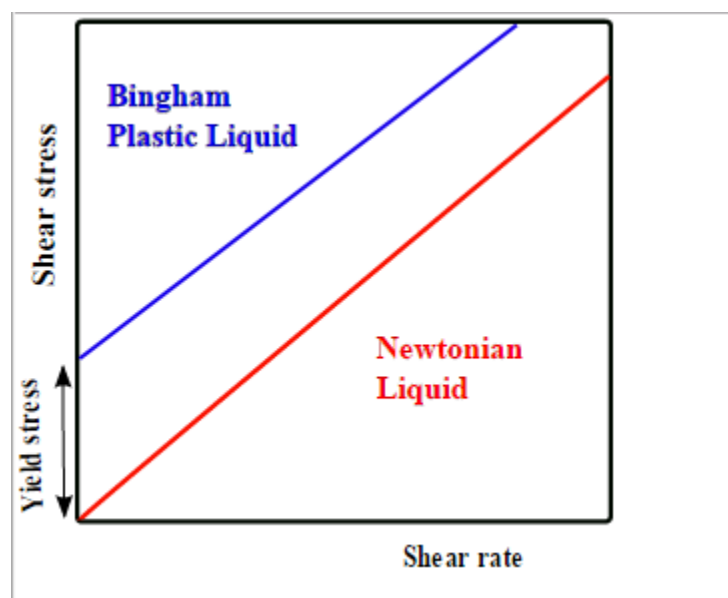


Figure D-1 Rheology Graph Contrasting Newtonian and Bingham Plastic Liquid.

- Heat transfer. Mixing is important in heat transfer for moving “hot” fluid away from the steam coils, hot glass in contact with mantles or heating rods and replacing it with “cooler” fluid. If vessels are mixed sufficiently to blend miscible liquids, they should be mixed sufficiently to not adversely impact heat transfer.



When scaling mixing, the recommended maximum scale up ratio is ten based on linear scale<sup>68</sup> (1,000 based on volume). The scale up ratio between the 220 L unit and the DWPF is six. The ratios between the other units are less than 10, also. In addition, an impeller Reynolds number,

$$N_{RE} = D_I^2 \text{ cm}^2 \times \frac{N}{60 \text{ sec/min}} \rho \frac{\text{g}}{\text{cm}^3} / \nu \text{ cP} \times 100 \text{ cP} / P$$

was calculated (Table D-1 for SRAT and Table D-2 for SME) to verify that at all scales the units are operating in the turbulent regime.

The test units and the DWPF were designed so that any miscible blending occurs quickly. If the blending occurs quickly, it should not adversely affect processes such as anion destruction or hydrogen generation and release.

Since the test units and DWPF contain insoluble solids, the mixing systems and mixing speed were designed to suspend the solids particles to allow representative sampling. The purpose of suspending the solid particles is for them to participate in a chemical reaction, suspending them off the vessel bottom is sufficient in each of the test vessels as well as the DWPF.

Since the SRAT and SME contain slurries that behave as Bingham plastic fluids, the mixing systems at all scales were designed to provide homogeneous mixing. If the mixing is homogeneous, there should be no differences between scales due to mixing.

#### Cavern Model<sup>69</sup>

Mixing of Bingham plastic fluids can be described by the cavern model.<sup>64-65</sup> Figure D-2 describes the cavern model.

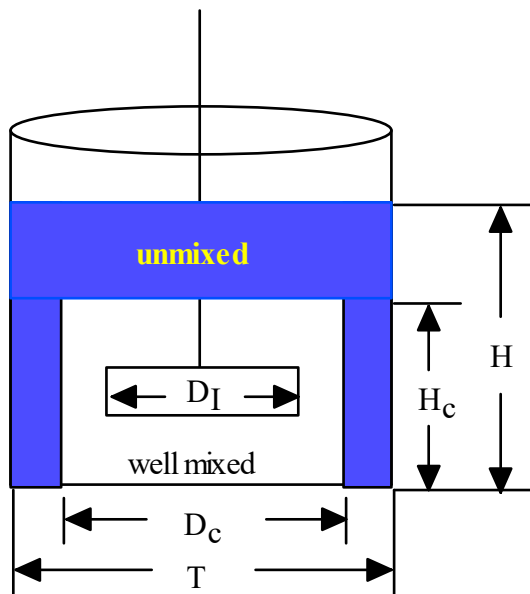


Figure D-2 Cavern Model.

For a cavern to form for a given impeller speed, the shear stresses generated by the impeller are greater than the yield stress of the slurry. The shape of the cavern is a right circular cylinder, in which the slurry is well mixed. In

areas outside of this cavern, where the slurry yield stress is larger than the shear stress generated at the cavern interface, the slurry remains motionless. This model assumes the fluid has constant physical properties throughout the vessel.

$$N_c = \frac{\pi}{D_I} \sqrt{\frac{\left(\frac{H_c}{D_c} + \frac{1}{3}\right) \left(\frac{T}{D_I}\right)^3 \tau_y}{\rho N_p}} \quad [1]$$

$$N_c = \sqrt{\frac{4V_c \pi \left(\frac{H_c}{D_c} + \frac{1}{3}\right) \tau_y}{\left(\frac{H_c}{D_c}\right) \rho N_p D_I^5}} \quad [2]$$

$$N_c = \sqrt{\frac{\left(\frac{T}{D_I}\right)^3 \pi^2 \tau_y}{1.32 N_p D_I^2}} \quad [3]$$

In equations [1] – [3],  $N_c$  is the impeller speed required for the cavern to reach the cylindrical walls of the vessel,  $V_c$  is the cavern volume,  $H_c$  is the cavern height,  $D_c$  is the cavern diameter,  $T$  is the tank diameter,  $D_I$  is the impeller diameter,  $\tau_y$  is the slurry yield stress,  $\rho$  is the slurry density, and  $N_p$  is the impeller power number (assumed to be 3). The height to diameter ratio of the cavern is based on the type of impeller, and is 0.4 for a disk turbine.<sup>65</sup> Once the cavern reaches the cylindrical walls of the vessel, the cavern height increases linearly with impeller speed until it reaches the top of the vessel.

Note that this analysis neglects the impact of boiling on mixing. Boiling causes gas vapor bubbles, which are buoyant and can help with vertical mixing and keeping solids suspended. So, mixing during processing is better than predicted by the above analysis. The data used for determining the mixing effectiveness are summarized in Table D-1 for SRAT and Table D-2 for SME.

**Table D-1 SRAT Mixing Dimensions and Calculated Mixing Parameters.**

Parameter	DWPF SRAT	IDMS	1/216	22-L	4-L	1-L
H <sub>c</sub> (cm)	499.872	281.305	83.312	32	29.591	19.9
D <sub>c</sub> (cm)	365.76	213.36	60.96	29.464	15.0114	10
D <sub>I</sub> (cm)	91.44	76.2	15.24	10.16	7.50	5.08
τ <sub>y</sub> (dynes/cm <sup>2</sup> )	50	50	50	50	50	50
Density (g/ml)	1.2	1.2	1.2	1.2	1.2	1.2
N <sub>p</sub> (dimensionless)	3	3	3	3	3	3
Viscosity, (cP)	12	12	12	12	12	12
Revolution Per Minute	130	156	250	375	500	750
N <sub>RE</sub> (dimensionless)	181,161	150,967	9,677	6,452	4,688	3,226
Equation 1	$N_c = \frac{\pi}{D_I} \sqrt{\frac{\left(\frac{H_c}{D_c} + \frac{1}{3}\right) \left(\frac{T}{D_I}\right)^3 \tau_y}{\rho N_p}}$					
N <sub>c</sub> (1/sec)	2.14	1.48	12.85	10.87	10.76	15.56
N <sub>c</sub> (rpm)	128	89	771	652	646	934
Equation 2	$N_c = \sqrt{\frac{4V_c \pi \left(\frac{H_c}{D_c} + \frac{1}{3}\right) \tau_y}{\left(\frac{H_c}{D_c}\right) \rho N_p D_I^5}}$					
N <sub>c</sub> (rps)	2.14	1.48	12.85	10.87	10.76	15.56
N <sub>c</sub> (rpm)	128	89	771	652	646	934
Equation 3	$N_c = \sqrt{\frac{\left(\frac{T}{D_I}\right)^3 \pi^2 \tau_y}{1.32 N_p D_I^2}}$					
N <sub>c</sub> (rps)	1.69	1.19	10.15	9.40	7.30	10.51
N <sub>c</sub> (rpm)	101	71	609	564	438	631
Average N <sub>c</sub> (rpm)	119	83	717	623	576	833
Power (hp)	5.6	0.76	0.16	0.013	0.0024	0.0010
Volume Calc (cc)	52,521,982	10,057,576	243,157	21,818	5,237	1,563
Volume (gal)	13,876	2,657	64.2	5.76	1.38	0.41
P/V (hp/1000 gal)	2.05	1.45	12.30	11.83	8.57	12.33
Tip Speed (ft/s)	18.8	10.9	18.8	10.9	7.4	7.3
Low Speed (rpm)	65	78	124	186	252	372
High Speed (rpm)	130	156	248	372	505	745
Low Tip Speed (cm/min)	5,944	5,944	5,944	5,944	5,944	5,944
High Tip Speed (cm/min)	11,887	11,887	11,887	11,887	11,887	11,887

**Table D-2 SME Mixing Dimensions and Calculated Mixing Parameters.**

Parameter	DWPF SRAT	IDMS	1/216	22-L	4-L	1-L
H <sub>c</sub> (cm)	499.872	281.305	83.312	32	29.591	19.9
D <sub>c</sub> (cm)	365.76	213.36	60.96	29.464	15.0114	10
DI (cm)	91.44	76.2	15.24	10.16	7.50	5.08
τ <sub>y</sub> (dynes/cm <sup>2</sup> )	150	150	150	150	150	150
Density (g/ml)	1.4	1.4	1.4	1.4	1.4	1.4
N <sub>p</sub>	3	3	3	3	3	3
Viscosity, cP	40	40	40	40	40	40
Revolution Per Minute	130	156	250	375	500	750
N <sub>Re</sub>	63,406	52,839	3,387	2,258	1,641	1,129
Equation 1	$N_c = \frac{\pi}{D_I} \sqrt{\frac{\left(\frac{H_c}{D_c} + \frac{1}{3}\right) \left(\frac{T}{D_I}\right)^3 \tau_y}{\rho N_p}}$					
N <sub>c</sub> (1/sec)	1.34	0.93	8.01	6.78	6.71	9.70
N <sub>c</sub> (rpm)	80	56	481	407	403	582
Equation 2	$N_c = \sqrt{\frac{4V_c \pi \left(\frac{H_c}{D_c} + \frac{1}{3}\right) \tau_y}{\left(\frac{H_c}{D_c}\right) \rho N_p D_I^5}}$					
N <sub>c</sub> (rps)	1.34	0.93	8.01	6.78	6.71	9.70
N <sub>c</sub> (rpm)	80	56	481	407	403	582
Equation 3	$N_c = \sqrt{\frac{\left(\frac{T}{D_I}\right)^3 \pi^2 \tau_y}{1.32 N_p D_I^2}}$					
N <sub>c</sub> (rps)	0.98	0.69	5.86	5.43	4.21	6.07
N <sub>c</sub> (rpm)	59	41	352	326	253	364
Average N <sub>c</sub> (rpm)	73	51	438	380	353	509
Power (hp)	28.4	3.85	0.79	0.068	0.0119	0.0051
Volume Calc (cc)	52,521,982	10,057,576	243,157	21,818	5,237	1,563
Volume (gal)	13,876	2,657	64.2	5.76	1.38	0.41
P/V (hp/1000 gal)	0.40	0.28	2.40	2.30	1.68	2.42
Tip Speed (ft/s)	11.5	6.6	11.5	6.6	4.5	4.4
Low Speed (rpm)	65	78	124	186	252	372
High Speed (rpm)	130	156	248	372	505	745
Low tip speed (cm/min)	5,944	5,944	5,944	5,944	5,944	5,944
High tip speed (cm/min)	11,887	11,887	11,887	11,887	11,887	11,887

**Distribution:**[timothy.brown@srnl.doe.gov](mailto:timothy.brown@srnl.doe.gov)[alex.cozzi@srnl.doe.gov](mailto:alex.cozzi@srnl.doe.gov)[gregg.morgan@srnl.doe.gov](mailto:gregg.morgan@srnl.doe.gov)[david.crowley@srnl.doe.gov](mailto:david.crowley@srnl.doe.gov)[a.fellinger@srnl.doe.gov](mailto:a.fellinger@srnl.doe.gov)[c.diprete@srnl.doe.gov](mailto:c.diprete@srnl.doe.gov)[samuel.fink@srnl.doe.gov](mailto:samuel.fink@srnl.doe.gov)[nancy.halverson@srnl.doe.gov](mailto:nancy.halverson@srnl.doe.gov)[erich.hansen@srnl.doe.gov](mailto:erich.hansen@srnl.doe.gov)[connie.herman@srnl.doe.gov](mailto:connie.herman@srnl.doe.gov)[Joseph.Manna@srnl.doe.gov](mailto:Joseph.Manna@srnl.doe.gov)[kevin.fox@srnl.doe.gov](mailto:kevin.fox@srnl.doe.gov)[john.mayer@srnl.doe.gov](mailto:john.mayer@srnl.doe.gov)[daniel.mccabe@srnl.doe.gov](mailto:daniel.mccabe@srnl.doe.gov)[frank.pennebaker@srnl.doe.gov](mailto:frank.pennebaker@srnl.doe.gov)[william.ramsey@srnl.doe.gov](mailto:william.ramsey@srnl.doe.gov)[michael.stone@srnl.doe.gov](mailto:michael.stone@srnl.doe.gov)[michael.poirier@srnl.doe.gov](mailto:michael.poirier@srnl.doe.gov)[boyd.wiedenman@srnl.doe.gov](mailto:boyd.wiedenman@srnl.doe.gov)[bill.wilmarth@srnl.doe.gov](mailto:bill.wilmarth@srnl.doe.gov)[chris.martino@srnl.doe.gov](mailto:chris.martino@srnl.doe.gov)[Amy.Ramsey@srnl.doe.gov](mailto:Amy.Ramsey@srnl.doe.gov)[jeffrey.crenshaw@srs.gov](mailto:jeffrey.crenshaw@srs.gov)[james.folk@srs.gov](mailto:james.folk@srs.gov)[roberto.gonzalez@srs.gov](mailto:roberto.gonzalez@srs.gov)[patrick.jackson@srs.gov](mailto:patrick.jackson@srs.gov)[tony.polk@srs.gov](mailto:tony.polk@srs.gov)[jean.ridley@srs.gov](mailto:jean.ridley@srs.gov)[patricia.suggs@srs.gov](mailto:patricia.suggs@srs.gov)[kevin.brotherton@srs.gov](mailto:kevin.brotherton@srs.gov)[richard.edwards@srs.gov](mailto:richard.edwards@srs.gov)[terri.fellinger@srs.gov](mailto:terri.fellinger@srs.gov)[eric.freed@srs.gov](mailto:eric.freed@srs.gov)[barbara.hamm@srs.gov](mailto:barbara.hamm@srs.gov)[bill.holtzscheiter@srs.gov](mailto:bill.holtzscheiter@srs.gov)[john.iaukea@srs.gov](mailto:john.iaukea@srs.gov)[vijay.jain@srs.gov](mailto:vijay.jain@srs.gov)[victoria.kmiec@srs.gov](mailto:victoria.kmiec@srs.gov)[Jeremiah.Ledbetter@srs.gov](mailto:Jeremiah.Ledbetter@srs.gov)[jeff.ray@srs.gov](mailto:jeff.ray@srs.gov)[paul.ryan@srs.gov](mailto:paul.ryan@srs.gov)[azadeh.samadi-dezfouli@srs.gov](mailto:azadeh.samadi-dezfouli@srs.gov)[hasmukh.shah@srs.gov](mailto:hasmukh.shah@srs.gov)[aaron.staub@srs.gov](mailto:aaron.staub@srs.gov)[christie.sudduth@srs.gov](mailto:christie.sudduth@srs.gov)[spencer.isom@srs.gov](mailto:spencer.isom@srs.gov)[lauryn.jamison@srs.gov](mailto:lauryn.jamison@srs.gov)[maria.rios-armstrong@srs.gov](mailto:maria.rios-armstrong@srs.gov)[thomas.colleran@srs.gov](mailto:thomas.colleran@srs.gov)[Jonathan.Bricker@srs.gov](mailto:Jonathan.Bricker@srs.gov)[david.sherburne@srs.gov](mailto:david.sherburne@srs.gov)[Helen.Boyd@srs.gov](mailto:Helen.Boyd@srs.gov)[Grace.Chen@srs.gov](mailto:Grace.Chen@srs.gov)[Mason.Clark@srs.gov](mailto:Mason.Clark@srs.gov)[jeffrey.gillam@srs.gov](mailto:jeffrey.gillam@srs.gov)[barbara.hamm@srs.gov](mailto:barbara.hamm@srs.gov)[Jocelin.Stevens@srs.gov](mailto:Jocelin.Stevens@srs.gov)[Records Administration \(EDWS\)](#)